Science Translational Medicine AAAS

Submitted Manuscript: Confidential template updated: February 28 2012

Title: An anti-inflammatory eicosanoid switch mediates the suppression of type-2 inflammation by helminth larval products

Authors: Marta de los Reyes Jiménez[1*], Antonie Lechner[1*], Francesca Alessandrini[1], Sina Bohnacker[1], Sonja Schindela[1], Aurélien Trompette[2], Pascal Haimerl[1], Dominique Thomas[3], Fiona Henkel[1], André Mourão[4], Arie Geerlof[4], Clarissa Prazeres da Costa[5], Adam M Chaker[6], Bernhard Brüne[7], Rolf Nüsing[7], Per-Johan Jakobsson[8], Wolfgang A Nockher[9], Matthias J Feige[10], Martin Haslbeck[11], Caspar Ohnmacht[1], Benjamin J Marsland[12], David Voehringer[13], Nicola L Harris[12], Carsten B Schmidt-Weber[1,14], Julia Esser-von Bieren[1#]

[*] These authors contributed equally

[#]To whom correspondence should be addressed: Julia.esser@helmholtz-muenchen.de

Affiliations:

[1]Center of Allergy and Environment (ZAUM), Technical University of Munich and Helmholtz Center Munich, 80802 Munich, Germany

[2]Faculty of Biology and Medicine, University of Lausanne, Service de Pneumologie, Centre Hospitalier Universitaire Vaudois, 1066 Epalinges, Switzerland

[3]Institute of Clinical Pharmacology, Goethe-University Frankfurt, 60590 Frankfurt am Main, Germany

[4]Protein Expression and Purification Facility (PEPF), Institute of Structural Biology, Helmholtz Center Munich, Germany

[5]Institute for Medical Microbiology, Immunology and Hygiene, Technical University of Munich, 81675 Munich, Germany

[6]Department of Otolaryngology, Allergy Section, Klinikum Rechts der Isar, Technical University of Munich, Munich, Germany

[7]Institute of Biochemistry I, Faculty of Medicine, Goethe-University Frankfurt, 60590 Frankfurt am Main, Germany

[8]Rheumatology Unit, Department of Medicine, Karolinska Institute Stockholm, 171 76 Stockholm, Sweden

[9]Institute of Laboratory Medicine and Pathobiochemistry, Molecular Diagnostics, Philipps-University Marburg, 35043 Marburg, Germany

[10]Center for Integrated Protein Science Munich at the Department of Chemistry and Institute for Advanced Study, Technical University of Munich, 85748 Garching, Germany

[11]Department of Chemistry, Technical University of Munich, 85748 Garching, Germany

[12]Department of Immunology and Pathology, Central Clinical School, Monash University, The Alfred Centre, Melbourne, VIC 3004, Australia

[13]Department of Infection Biology, University Hospital Center, Friedrich-Alexander University, Erlangen-Nuremberg, Germany

[14]Member of the German Center of Lung Research (DZL)

Abstract: Eicosanoids are key mediators of type-2 inflammation, e.g. in allergy and asthma. Helminth products have been suggested as remedies against inflammatory diseases, but their effects on eicosanoids have remained elusive. Here, we show that larval products of the helminth *Heligmosomoides polygyrus bakery* (*HpbE*) trigger a broad anti-inflammatory eicosanoid shift by suppressing the 5-lipoxygenase-, but inducing the cyclooxygenase (COX) pathway. In human macrophages and granulocytes, the *HpbE*-driven induction of the COX pathway resulted in the production of anti-inflammatory mediators (e.g. prostaglandin E_2 (PGE_2) and IL-10) and suppressed chemotaxis. Intranasal treatment with *HpbE* extract attenuated allergic airway inflammation in mice and intranasal transfer of *HpbE*-conditioned macrophages led to reduced airway eosinophilia in a COX/PGE_2-dependent fashion. The induction of regulatory mediators in macrophages depended on p38 MAPK, hypoxia inducible factor-1 alpha (HIF-1α) and *Hpb* glutamate dehydrogenase (*Hpb* GDH), which we identify as a major immune regulatory protein in *HpbE*. *Hpb* GDH activity was required for anti-inflammatory effects of *HpbE* in macrophages and local administration of recombinant *Hpb* GDH to the airways abrogated allergic airway inflammation in mice. Thus, a metabolic enzyme present in helminth larvae can suppress type-2 inflammation by inducing an anti-inflammatory eicosanoid switch, which has important implications for the therapy of allergy and asthma.

One Sentence Summary: A helminth larval extract and its component *Hpb* glutamate dehydrogenase induce an anti-inflammatory mediator switch to suppress type-2 inflammation.

Introduction

Severe type-2 inflammation, e.g. in asthma or nasal polyposis represents a major clinical need, which is insufficiently targeted by current treatments *(1–3)*. Eicosanoids are bioactive metabolites of the polyunsaturated fatty acid (PUFA) arachidonic acid (AA), which play major roles in severe and therapy-resistant forms of type-2 inflammation *(4, 5)*. However, current therapeutics fail to sufficiently modulate eicosanoid pathways *(6)*, resulting in poor clinical efficacy against asthma and nasal polyps *(3, 7)*.

Among the eicosanoids, leukotrienes (LTs), formed via the 5-lipoxygenase (5-LOX) pathway, as well as the cyclooxygenase (COX) metabolite prostaglandin D_2 (PGD_2) are the key drivers of type-2 inflammation *(8–10)*. In contrast, prostaglandin E_2 (PGE_2) and prostacyclin (PGI_2) can suppress allergic inflammation and asthma symptoms *(11–14)*. Recently, eicosanoids have also been suggested to participate in the type-2 immune response to helminth parasites *(15, 16)*.

Infection with helminths, tissue damage or exposure to allergens can trigger type-2 immune responses, which - if not properly controlled - can result in chronic type-2 inflammation *(17)*. However, helminths can also counter-regulate type-2 immune responses, e.g. by inducing regulatory T cells or by targeting innate effector mechanisms, such as IL-33, type-2 innate lymphoid cells (ILC2s) or M2 macrophages *(18–21)*. *H. polygyrus bakeri* (*Hpb*) is a natural parasite of mice with particularly potent regulatory effects on type-2 immune responses. Products of adult *Hpb* worms can suppress allergic airway inflammation in mice *(20, 21)* and *Hpb* larvae can interfere with the innate type-2 immune response that is initiated early after infection *(22)*. Based on their potent immune regulatory potential, helminth products have been suggested as remedies for inflammatory diseases, including allergy and asthma *(19, 23)*.

However, if helminth products can modulate eicosanoid pathways and thus interfere with type-2 inflammation, had not been studied.

Results

Treatment with Hpb larval extract suppresses allergic airway inflammation in vivo

Hpb larvae modulate innate type-2 immunity *(22)* and eicosanoids are a critical innate component of the type-2 immune response to house dust mite (HDM) *(8, 13, 24)*. Thus, we hypothesized that *Hpb* larvae may produce factors, which modulate eicosanoid-driven type-2 inflammation. To mimic a desirable therapeutic application, we administered an extract of infective *Hpb* L3 larvae (*HpbE*) topically (intranasally, i.n.) during HDM-induced allergic airway inflammation *in vivo* (Fig. 1a). Indeed, intranasal treatment with *HpbE* reduced hallmarks of type-2 inflammation, including airway eosinophilia, goblet cell hyperplasia and mucin maturation (Fig. 1b,c). Consistent with increased eosinophil numbers, 15-HETE, a major AA metabolite of eosinophils was increased in bronchoalveolar lavage fluid (BALF) of HDM-sensitized mice and treatment with *HpbE* decreased 15-HETE as well as pro-inflammatory cytokines and chemokines (IL-5, IL-6, Eotaxin, RANTES) (Fig. 1d). Hence, topical treatment with *HpbE* could suppress the inflammatory response to HDM in the airways.

HpbE-treated macrophages produce reduced levels of leukotrienes and modulate allergic airway inflammation via prostaglandin E_2

Genetic ablation or pharmacological inhibition of eicosanoid pathways affects the development of allergic airway inflammation itself, thus impeding the assessment of *HpbE* effects in such

models *(8, 13, 25)*. However, macrophage transfer experiments can provide valuable insights into the role of eicosanoids in allergic airway inflammation *(12)* as macrophages represent particularly plastic eicosanoid producing cells that determine the inflammatory response to HDM in the airways *(24, 26)*.

First, we characterized the eicosanoid profile of *HpbE*-treated bone marrow-derived macrophages (BMDM) by LC-MS/MS. In order to elicit AA release and analyze the full capacity of eicosanoid formation, cells were stimulated with ionophore (A23187). Consistent with the anti-inflammatory potential of *HpbE*, we observed a shift from type-2-inducing metabolites (PGD_2, LTs) to regulatory metabolites (PGE_2) after treatment with *HpbE* (Fig. 2a). This shift was most likely a result of transcriptional changes in AA-metabolizing enzymes as *HpbE* induced COX-2 (gene: *Ptgs2*) and microsomal prostaglandin E synthase (mPGES-1, gene: *Ptges*), whilst suppressing 5-LOX (*Alox5*) and leukotriene C_4 synthase (*Ltc4s*) gene expression (Fig. 2b).

To investigate whether the eicosanoid-modulatory effects of *HpbE* could be translated to human macrophages, we treated human monocyte-derived macrophages (MDM) with *HpbE* and assessed their lipid mediator profile after stimulation with A23187. Using an LC-MS/MS eicosanoid screen (including 200 different eicosanoids and PUFAs (table S1)), we confirmed that *HpbE* treatment resulted in fundamental changes in PUFA metabolites with the largest changes observed for COX metabolites (Fig. 2c, fig. S1a,b). Whilst PGE_2, TXB_2 and 12-hydroxyheptadecatrenoic acid (12-HHT) were increased, *HpbE* tended to reduce the production of pro-inflammatory 5-LOX metabolites (LTB_4 and LTC_4), but to enhance the synthesis of the pro-resolving mediator lipoxin A_5 (LXA_5) (Fig. 2c,d). Thus, *HpbE* induced a broad and potentially anti-inflammatory eicosanoid switch.

In line with *HpbE*-induced transcriptional changes in BMDM, human macrophages responded to *HpbE* by inducing the expression of enzymes involved in the biosynthesis of PGE_2: *PTGS2* (COX-2) and *PTGES* (mPGES-1) (Fig. 2e). In contrast, *HpbE* reduced the expression of *PTGDS* (prostaglandin D_2 synthase) as well as of LT biosynthetic enzymes: *ALOX5*, *LTA4H* (leukotriene A_4 hydrolase) and *LTC4S* and the high affinity receptor for cysLTs (cysteinyl leukotriene receptor-1, *CYSLTR1*) (Fig. 2e). Taken together, *HpbE* triggered a switch from a pro-inflammatory 5-LOX-dominated to a type-2-suppressive COX-dominated eicosanoid profile.

To define the *in vivo* relevance of the *HpbE*-driven induction of COX metabolites in macrophages, we intranasally transferred BMDM from wildtype (wt), COX-2 (*Ptgs2*$^{-/-}$) or mPGES-1 (*Ptges*$^{-/-}$) deficient mice during HDM-induced airway inflammation. Transfer of untreated wt BMDM tended to increase eosinophil frequencies in the airways of HDM-sensitized mice, an effect that was reversed by transfer of *HpbE*-treated wt BMDM (Fig. 2f,g).

In addition, mice that received *HpbE*-treated wt BMDM during challenges with HDM showed reduced eosinophil numbers and airway inflammation as compared to mice that received untreated wt BMDM (Fig. 2f,g). In contrast, *HpbE*-treated or untreated *Ptges*$^{-/-}$ BMDM similarly affected eosinophil numbers in BALF and eosinophilic airway inflammation tended to be increased after transfer of *HpbE*-treated compared to untreated *Ptges*$^{-/-}$ BMDM (Fig. 2f,g). Finally, *HpbE*-treated *Ptgs2*$^{-/-}$ BMDM transfer led to exaggerated HDM-induced airway inflammation (fig. S1c). This suggested that macrophage-derived COX metabolites, particularly mPGES-1-derived PGE_2, can contribute to the anti-inflammatory effects of *HpbE in vivo*.

HpbE induces type-2-suppressive cytokines and prevents M2 polarization

To investigate whether treatment with *HpbE* also modified cytokine profiles and the polarization of macrophages, we quantified cytokines implicated in macrophage polarization and the regulation of type-2 inflammation. Treatment of human MDM with *HpbE* resulted in the induction of IL-10, IL-1β, IL-12, IL-18, IL-27 and TNF-α, all known to modulate M2 polarization and type-2 immune responses (Fig. 3a,b) *(22, 27–31)*. However, *HpbE* hardly affected the production of mediators of type-2 inflammation (IL-33 or CCL17) by macrophages (Fig. 3b). The *HpbE*-triggered induction of IL-10 and IL-1β also occurred in murine BMDM, albeit at 10-100fold lower amplitude as compared to human MDM (Fig. 3c).

In addition, *HpbE* downregulated the expression of M2 markers (*ALOX15* (15-Lipoxygenase, 15-LOX) and *MRC1* (Mannose Receptor C-Type 1, MR/ CD206)), but not transglutaminase-2 (*TGM2*) in human MDM, suggesting that it could partially counteract M2 polarization (Fig. 3d). As human and mouse M2 macrophages are defined by distinct sets of markers *(32)*, we also investigated the effect of *HpbE* on murine M2 polarization. As in human MDM, *HpbE* tended to downregulate *Mrc1* in mouse BMDM. In contrast, *Tgm2* and *Arg1* expression rather increased, whilst *Tmed1*/ *St2l* and *Retnla*/ *Fizz1* remained unaffected by *HpbE* (Fig. 3e). Together, these data suggest that *HpbE* can broadly modulate the polarization and mediator output of human macrophages to induce a regulatory, type-2-suppressive phenotype.

HpbE has a unique potential to induce type-2 suppressive mediators

For the treatment of complex type-2 inflammatory diseases such as allergy, asthma and nasal polyps, regulation of multiple pathways is often superior to targeting single mechanisms. Indeed, GCs, which regulate a broad array of inflammatory pathways are widely used in the treatment of these diseases and still represent the first-line therapy for most patients. Thus, we compared the

immune regulatory effects of *HpbE* to those of GCs (dexamethasone (Dex) and fluticasone propionate (FP)) with a focus on eicosanoid pathways and the anti-inflammatory cytokine IL-10. Whilst *HpbE* triggered a shift from pro-inflammatory genes (*ALOX5*, *LTC4S*, *PTGDS*) and 5-LOX metabolites to anti-inflammatory pathways (*PTGS2*, *PTGES*, PGE_2, IL-10), GCs tended to enhance *LTC4S* expression and to suppress PGE_2 synthesis in macrophages (fig. S2a-c).

In human granulocytes (PMN), which also represent an important source of eicosanoids, *HpbE* and FP, but not Dex, tended to reduce pro-inflammatory metabolites of AA and linoleic acid (LA) *(33)* (fig. S2d). Together, this suggested that compared to GCs, *HpbE* is more efficient in inducing a regulatory mediator profile that can counteract type-2 inflammation.

As larval stages of *S. mansoni* (*S.m.*) as well as excretory secretory products of *Hpb* adult stages (HES) can induce type-2-suppressive mediators *(34, 35)*, we compared *S.m.*- or HES-elicited effects on eicosanoids and IL-10 to those of *HpbE*. An extract of *S.m.* larvae (*SmE*) failed to induce a shift from 5-LOX to COX metabolism and was less potent in triggering IL-10 production as compared to *HpbE* (fig. S3a,b). Similarly, adult-stage HES failed to induce the COX pathway as well as IL-10 (fig. S3c,d). In addition, extracts of L4 and L5 stages of *Hpb* did not show any induction of PGE_2 and exhibited only minor suppressive effects on cysLTs as compared to L3 stage extract (*HpbE*) (fig. S3e). In contrast to L3 extract, L4 and L5 extracts did not induce type-2 suppressive cytokines (IL-1β and IL-10; fig. S3e).

As changes in the microbiota contribute to the suppression of type-2 inflammation by *Hpb* infection *(36)*, we further identified *HpbE*-associated bacteria and assessed whether these would exert similar effects as *HpbE*. However, COX metabolites, IL-10 and COX-pathway genes remained unaffected by treatment with *HpbE*-associated bacteria (fig. S3f,g). To further exclude that the *HpbE*-triggered induction of regulatory mediators was due to LPS contamination, we

additionally quantified mediator profiles of macrophages treated with LPS at the concentration present in *HpbE* (60 ng/ml). However, LPS alone failed to significantly induce COX metabolites (fig. S3h). Together this suggested that *HpbE* has a unique immune regulatory profile, which is distinct from GCs and somatic extracts from *S. mansoni* larvae or more mature stages of *Hpb* as well as from *Hpb*-associated bacteria.

HpbE modulates eicosanoid production and chemotaxis of human granulocytes

Together with macrophages, granulocytes represent a major source of eicosanoids during type-2 inflammation. Thus, we determined whether *HpbE* would affect the PUFA metabolism of human granulocytes by LC-MS/MS analysis. To limit apoptosis and mimic an inflammatory setting, granulocytes were cultured in the presence of GM-CSF, which resulted in 40-50% viability after 24h. Treatment with *HpbE* significantly reduced neutrophil viability, but had no effect on the viability of eosinophils (fig. S4a). We confirmed that neutrophils and eosinophils show abundant expression of LT-biosynthetic enzymes (*ALOX5*, *LTA4H, LTC4S)* at baseline, allowing them to synthesize high levels of LTs upon ionophore stimulation (Fig. 4a-e, fig. S4b) *(37)*. In line with the profiles observed for macrophages, granulocytes showed an induction of COX metabolites (particularly 12-HHT and TXB_2) after treatment with *HpbE* (Fig. 4a,b, fig. S4c). Furthermore, the levels of 5-LOX metabolites were reduced by *HpbE* treatment in ionophore-stimulated mixed human granulocytes as well as in purified eosinophils (Fig. 4b,c). Similar to *HpbE*-driven changes in AA metabolism genes in macrophages, enzymes involved in the synthesis of pro-inflammatory mediators (*ALOX5*, *LTA4H* and *PTGDS*) were downregulated, whilst *PTGS2* and *PTGES* were induced by *HpbE* in human granulocytes (Fig. 4d,e).

Eicosanoid-driven granulocyte recruitment represents a key event in type-2 inflammation *(5, 8)*. Thus, we studied how *HpbE* would affect granulocyte recruitment in a clinically relevant setting of type-2 inflammation, in which AA metabolites play a major role. We collected granulocytes and nasal polyp secretions from patients suffering from Aspirin exacerbated respiratory disease (AERD) and assessed the effects of *HpbE* on the migration of patient granulocytes towards nasal polyp secretions *ex vivo*. Pre-treatment of AERD granulocytes with *HpbE* resulted in a marked reduction in cell recruitment, an effect not achieved by fluticasone propionate or the cysLT1R antagonist Montelukast (MK), which are commonly used to treat AERD symptoms (Fig. 4f). In keeping with the suppression of granulocyte chemotaxis, *HpbE* reduced surface levels of chemotactic receptors (C-C chemokine receptor type 3 (CCR3) and PGD_2 receptor 2 ($CRTH_2$)) on human eosinophils (Fig. 4g). To investigate whether COX metabolites released by *HpbE*-treated human macrophages could impact on granulocyte recruitment, we performed chemotaxis assays in the presence of conditioned media from MDM treated with *HpbE* and the non-selective COX-inhibitor indomethacin. In line with our *in vivo* data (Fig. 2f,g), conditioned media from *HpbE*-treated human macrophages reduced granulocyte chemotaxis and indomethacin partially restored cell recruitment (Fig. 4h). Thus, either directly or by acting on macrophages, *HpbE* can suppress the chemotaxis of granulocytes, including those from patients suffering from severe type-2 inflammation.

HpbE induces IFN-γ, IL-10 and an anti-inflammatory eicosanoid switch in human PBMCs

To test whether the regulatory potential of *HpbE* extended to type-2 cytokines, we analyzed IL-4, IL-5 and IL-13 expression in human peripheral blood mononuclear cells (PBMCs) after treatment with *HpbE*. Type-2 cytokines were hardly affected by *HpbE*, which instead triggered a

marked induction of IFN-γ and IL-10 (fig. S5a,b). In line with eicosanoid modulation in macrophages and granulocytes, *HpbE* treatment of PBMCs also triggered the synthesis of prostanoids (PGE_2 and TXB_2), whilst decreasing 5-LOX metabolites (5-HETE, and LTB_4) (fig. S5c). However, in contrast to macrophages and granulocytes, *HpbE*-treated PBMCs produced high levels of 12-/15-LOX metabolites (fig. S5c), which can be metabolized into pro-resolving mediators *(38)*. The modulation of IL-10 and eicosanoids in PBMCs was entirely dependent on $CD14^+$ monocytes as $CD14^-$ PBMCs produced low levels of these mediators with no apparent regulation by *HpbE* (fig. S5d). Thus, *HpbE* acted predominantly on monocytes/ macrophages to induce a regulatory and potentially pro-resolving eicosanoid profile.

The HpbE-induced regulatory eicosanoid switch depends on HIF-1α

To identify mechanisms by which *HpbE* could trigger the production of type-2-suppressive mediators, we targeted regulatory pathways genetically or pharmacologically and studied eicosanoid profiles and macrophage polarization. As HIF-1α is a positive regulator of the COX pathway *(39)*, we first assessed the effect of *HpbE* on HIF-1α activation and COX-2 expression in BMDM. After treatment with *HpbE*, nuclear translocation of HIF-1α, and expression of COX-2 were increased (Fig. 5a). In contrast to wildtype BMDM, HIF-1α deficient BMDM ($HIF\text{-}1\alpha^{fl/fl}$xLysMCre) failed to upregulate TXB_2 and PGE_2 in response to *HpbE*, while the suppression of (PGD_2 and LTB_4) remained intact (Fig. 5b). In addition, HIF-1α deficient BMDM showed a reduced *HpbE*-driven induction of IL-6, TNFα and IL-10 as well as of the M2 markers *Tgm2* and *Arg1* (Fig. 5c,d). Levels of *Mrc1* and *Retnla* were generally higher in BMDM lacking HIF-1α, but *HpbE* down-regulated *Mrc1* expression regardless of HIF-1α (Fig. 5d). Thus, the induction of type-2-suppressive mediators in BMDM was largely dependent on HIF-1α.

As HIF-1α is positively regulated by the p38 MAPK, we studied the involvement of p38 signaling in the induction of type-2-suppressive mediators by *HpbE*. In human MDM, p38 was phosphorylated upon treatment with *HpbE*, correlating with the induction of COX-2 (Fig. 5e) and a p38 inhibitor (VX-702) abrogated the induction of IL-10, IL-1β and PGE_2-synthetic enzymes (*PTGS2* and *PTGES*) (Fig. 5f-h). In line with HIF-1α dependent regulation in murine BMDM, a pharmacological inhibitor of HIF-1α (acriflavine) attenuated the *HpbE*-induced expression of IL-10, IL-1β and COX pathway enzymes in human MDM (Fig. 5f-h). However, p38 and HIF-1α were not responsible for the modulation of the 5-LOX pathway (Fig. 5h).

Inhibition of the COX pathway abrogates the induction of type-2-suppressive mediators by HpbE

To investigate whether the *HpbE*-triggered production of IL-10 and IL-1β occurred downstream of the COX pathway, we studied whether COX inhibitors could modify the induction of these cytokines. A non-selective COX inhibitor (indomethacin), but not a selective COX-2 inhibitor (CAY10404) reduced the induction of IL-10, IL-1β and *PTGES* (Fig. 5f-h, fig. S6a,b). In contrast, the *HpbE*-triggered expression of COX-2 was reduced by both indomethacin as well as by selective inhibition of COX-2, suggesting that COX-2 metabolites could drive an autocrine feedback loop to promote COX-2 expression (Fig. 5h, fig. S6b).

As the transcription factor NF-κB and the kinases PI3 kinase, protein kinase A and PTEN can regulate eicosanoid pathways, we additionally assessed the contribution of these mechanisms to the induction of type-2-suppressive mediators by *HpbE*. Inhibition of NFκB (by BAY 11-7085) significantly reduced PGE_2, IL-10 and IL-1β production as well as gene expression of PGE_2-synthetic enzymes and IL-10 in *HpbE*-treated human MDM (fig. S6c,d). In contrast, inhibitors of PI3 kinase, protein kinase A or PTEN did not interfere with the induction of PGE_2, IL-10 or IL-

1β (fig. S6e). Thus, the *HpbE*-driven induction of type-2-suppressive mediators largely depended on the activation of p-38 MAPK, HIF-1α, NFκB and the COX pathway.

TLR2, dectin-1 and dectin-2 contribute to the induction of the COX pathway by HpbE

To further elucidate the upstream mechanisms underlying prostanoid- and cytokine modulation by *HpbE*, we blocked IL-1β or pattern recognition receptors (PRRs; TLR2, dectins-1/ 2), which had all been previously linked to helminth-driven immuneregulation *(15, 22, 40, 41)*. Blockade of IL-1β neither affected the *HpbE*-driven modulation of IL-10 nor of eicosanoid pathways (fig. S7a). However, neutralizing antibodies against TLR2, dectin-1 or dectin-2 reduced the induction of PGE_2-synthetic enzymes by *HpbE*, whilst the modulation of IL-10 or 5-LOX was not affected (fig. S7a,b). This suggested that TLR2 and dectins-1 and -2 contributed to the induction of the COX pathway, but not to other immune regulatory effects by *HpbE*.

Glutamate dehydrogenase is a major immune regulatory protein in HpbE

As the above-defined mechanisms did not provide a molecular explanation for the immune regulatory effects of *HpbE*, we further characterized its active components. Heat-inactivation of *HpbE* attenuated the induction of prostanoids, IL-10 and IL-1β in MDM as well as the *HpbE*-driven suppression of granulocyte recruitment (Fig. 6a,b). In addition, the induction of IL-10 by *HpbE* was abrogated if the extract was pre-treated with proteinase K (Fig. 6c). This suggested that the induction of type-2-suppressive mediators by *HpbE* was largely dependent on heat-labile and proteinase K digestible molecules, most likely proteins.

In order to identify immune regulatory proteins present in *HpbE*, we fractionated the extract by size exclusion chromatography and identified active fractions based on the capacity to induce the

COX metabolite TXB_2 as well as IL-10 (Fig. 6d,e). We then identified proteins present in active and non-active fractions by mass spectrometry. *Hpb* glutamate dehydrogenase (GDH) was uniquely present in active fractions of *HpbE,* qualifying it as an immune regulatory candidate (Fig. 6f, table S2). Indeed, an inhibitor of GDH (bithionol), which is also used as an anti-helminthic, reduced the *HpbE*-triggered induction of prostanoids and IL-10 in a dose-dependent manner without affecting cell viability (Fig. 6g,h, fig. S8a). In line with the unique anti-inflammatory properties of L3 (*HpbE*) *vs.* L4 and L5 extracts (fig. S3e), *HpbE* showed higher GDH activity as compared to L4 and L5 preparations (fig. S8b)

To further validate *Hpb* GDH as a major immune regulatory component of *HpbE*, we generated monoclonal antibodies (mABs) specific for *Hpb* GDH (i.e. not cross-reactive with mammalian (human/ mouse) GDH) (fig. S9A, S10). Indeed, administration of an anti-*Hpb* GDH antibody (clone 4F8), but not an isotype control antibody, resulted in a dose-dependent reduction of the *HpbE*-induced production of IL-10 and PGE_2 in human MDM (Fig. 6i, fig. S9B).

Recombinant Hpb glutamate dehydrogenase reduces allergic airway inflammation in vivo

Finally, we developed a strategy for the recombinant production of *Hpb* GDH, allowing us to directly assess immune regulatory effects of the protein *in vitro* and *in vivo*. Recombinant *Hpb* GDH was active and its activity was partially inhibited by bithionol (fig. S8c). In human MDM, treatment with *Hpb* GDH induced PGE_2 and IL-10, but reduced cysLT production, thus recapitulating key anti-inflammatory effects of total *HpbE* (Fig. 7a).

To validate the use as a potential therapeutic enzyme *in vivo*, mice were treated i.n. with *Hpb* GDH during HDM-induced allergic airway inflammation. Administration of *Hpb* GDH

attenuated the HDM-triggered eosinophil infiltration and airway inflammation as well as goblet cell hyperplasia and mucin maturation (Figs 7b,c).

Taken together, we identify *Hpb* GDH as a major immune regulatory protein in *HpbE* and thus a candidate for pre-clinical development as a new biologic for type-2 inflammation.

Discussion

Eicosanoids are central mediators of allergic inflammation *(8, 10, 25)* and type-2 immunopathology *(5, 42)*. Searching for new approaches to target eicosanoids in type-2 inflammation, we identified an extract of a parasitic nematode (*Heligmosomoides polygyrus bakeri*, *HpbE*) and its active component *Hpb* GDH, which exhibited unique eicosanoid-modulatory properties. *HpbE* showed broad immune regulatory effects in various myeloid cell types and when administered topically to the airways of allergen-sensitized mice. In a human *ex vivo* setting of type-2 inflammation, *HpbE* effectively reduced the chemotaxis of granulocytes towards nasal polyp secretions. The effects of *HpbE* on the chemotaxis of granulocytes from Aspirin-exacerbated respiratory disease (AERD) patients were particularly striking as this disease is characterized by an aberrant AA-metabolism and -signaling as well as GC-resistant type-2 inflammation *(5)*.

Of note, *HpbE* (although derived from a murine parasite) showed largely overlapping anti-inflammatory effects on eicosanoids and granulocyte activation in human cells *ex vivo* and in mice *in vivo*. *HpbE* likely impacted on granulocytes directly (e.g. by modulating eicosanoids and chemotactic receptors) as well as indirectly by inducing granulocyte-regulatory factors such as PGE_2 in macrophages. Although also other cell types can contribute to eicosanoid production during allergic airway inflammation, we focused on macrophages as a particularly plastic, long-

lived and thus therapeutically accessible source of these mediators. Indeed, the macrophage pool in inflamed airways consists of resident and infiltrating monocyte-derived cells, which develop into alveolar macrophages under the control of GM-CSF and TGFβ1 in the lung microenvironment *(43, 44)*. Thus, although the bone marrow- and monocyte-derived macrophages used in this study may not entirely reflect airway macrophages, they likely represent a relevant model for infiltrating, inflammatory monocytes, which crucially contribute to allergic airway inflammation *(26)*.

When treated with *HpbE* or *Hpb* GDH, monocytes and macrophages produced high levels of regulatory prostanoids, which can modulate type-2 immune responses by activating a regulatory macrophage phenotype and limiting type-2 cytokine production *(12, 45, 46)*. In contrast, eicosanoid pathways that typically drive type-2 inflammation (5-LOX/LTs, PTGDS/PGD_2) were suppressed by treatment with *HpbE* or *Hpb* GDH. *HpbE* also triggered the production of TXB_2, a mediator involved in platelet- and vascular function as well as tissue repair. Thus, in addition to modulating type-2 inflammation, helminth-induced eicosanoids may limit bleeding and tissue damage. Given the broad eicosanoid-modulatory potential of *HpbE* and *Hpb* GDH, it appears unlikely that only one metabolite or receptor is responsible for their anti-inflammatory effects. The finding that transfer of *HpbE*-conditioned wt but not *Ptges*$^{-/-}$ BMDM resulted in reduced eosinophilic airway inflammation as compared to transfer of untreated BMDM of the same genotype suggests that macrophage-derived PGE_2 may contribute to *HpbE*-driven immune regulation. In addition, the exaggerated allergic airway inflammation observed after transfer of *HpbE*-conditioned *Ptgs2*$^{-/-}$ BMDM supports a role for macrophage-derived COX metabolites, including PGE_2, in the anti-inflammatory effects of *HpbE*.

However, as we only obtained limited numbers of *Ptgs2*$^{-/-}$ BMDM and could thus not transfer untreated cells of this genotype, the strong inflammation observed after transfer of *HpbE*-conditioned *Ptgs2*$^{-/-}$ BMDM may also be due to COX-2 deficiency per se. Indeed, transfer of *Ptges*$^{-/-}$ BMDM led to reduced HDM-induced airway inflammation regardless of *HpbE*-conditioning. Thus, when transferred into an inflammatory environment, mPGES-1/COX-2 deficient BMDM may respond differently as compared to wt BMDM. Of note, when transferred into the airways during HDM challenge, untreated wt BMDM tended to increase eosinophilic inflammation, possibly due to HDM-induced chemokine production by the transferred macrophages *(47)*. In combination with the COX-dependent reduction of human granulocyte chemotaxis, the BMDM transfer data support an important role for macrophage-derived COX metabolites in the modulation of granulocyte responses during type-2 inflammation.

Indeed, to achieve therapeutic efficacy in allergy, asthma or nasal polyposis, the modulation of multiple eicosanoid pathways (e.g. cysLTs, PGD_2, PGE_2) may be favorable as targeting single pathways has failed to provide a significant clinical benefit *(7, 48)*. Although the 5-LOX pathway represents a key drug target in multiple chronic diseases, there are currently no known drugs that work by simultaneously preventing LT generation and inducing anti-inflammatory eicosanoids. The regulatory eicosanoid switch triggered by *HpbE* and its active component *Hpb* GDH thus represents a key asset compared to current anti-inflammatory drugs.

Given that nematode larvae (*C. elegans* and *N. brasiliensis*) had been reported to induce LT production and eosinophil recruitment, the LT-suppressive effects of *HpbE* were unexpected *(16, 47)*. However, our findings suggest that distinct helminth species and stages may differentially affect eicosanoid pathways and thus either promote or suppress type-2 inflammation. Indeed, we

observed that a larval extract of *S. mansoni* or extracts of L4 and L5 stages of *Hpb* failed to induce a shift from 5-LOX- to COX metabolism.

To potentially harness the eicosanoid-modulatory effects of *HpbE* and *Hpb* GDH, we chose a topical administration in a model of HDM-induced allergic airway inflammation, where the central role of prostanoids and LTs is well-documented *(6, 8, 12)*. Intranasal treatment with *HpbE* or *Hpb* GDH attenuated hallmarks of HDM-induced type-2 inflammation. This was in line with previous studies, showing that *Hpb* infection or treatment with excretory secretory products from the *Hpb* adult stage ("HES") can suppress allergic inflammation by modulating type-2 cytokine responses *(20, 34, 49)*. However, in comparison to HES, *HpbE* and *Hpb* GDH showed a unique potency to induce PGE_2 and IL-10, which can act in concert to induce regulatory macrophages and suppress type-2 inflammation *(12)*. Indeed, *HpbE* appeared to preferentially target early, innate immune mechanisms (e.g. granulocyte recruitment), whilst HES can modulate adaptive type-2 immune responses, e.g. by inducing regulatory T-cells *(18)*. *HpbE* or *Hpb* GDH may thus be particularly suited to target eicosanoids and myeloid cells as crucial innate components of type-2 inflammation.

Recently, protein components of HES (HpARI and Hp-TGM) have been identified as major immune regulatory factors *(20, 50)*. Particularly, HpARI and the hookworm protein AIP-2 were shown to have potent allergy-suppressive effects *(19, 20)*, but their effects on eicosanoids have not been studied. Using fractionation and mass-spectrometry, the enzyme *Hpb* GDH was identified as a major immune regulatory candidate in *HpbE*. Indeed, recombinant *Hpb* GDH could recapitulate all major anti-inflammatory effects of total *HpbE in vitro* and *in vivo*, suggesting a potential use as a novel therapeutic enzyme. However, as *Hpb* GDH only shows 60% identity to human GDH, immunogenicity may represent a limitation to its clinical

development as a new biotherapeutic. Thus, future studies should assess whether treatment with *Hpb* GDH results in the generation of neutralizing antibodies and design strategies to reduce the immunogenicity of the protein.

In addition, it will be important to define the mechanism of action by which *Hpb* GDH exerts its effects on eicosanoid pathways. Indeed, several PRRs (TLR2, dectin-1/2) participated in the induction of PGE_2-synthetic enzymes by *HpbE*. As TLR2 and dectins bind to carbohydrate structures the full immune regulatory potential of *HpbE* might rely on co-factors (e.g. carbohydrates or glycoproteins), which may act in concert with *Hpb* GDH or promote its activity. Based on its sequence, the natural, worm-derived *Hpb* GDH may also be O-glycosylated, which may result in recognition by C-type lectins and contribute to the immune regulatory activities of *HpbE*. This would be in line with a recent study, showing dectin-dependent induction of PGE_2 in dendritic cells by *Schistosoma* egg antigens *(15)*. However, recombinant *Hpb* GDH from *E. coli*, which is most likely not glycosylated, was also immunologically active, suggesting that glycosylation is not the major factor determining its immune regulatory activity.

In keeping with anti-inflammatory roles for myeloid NF-κB and HIF-1α in airway inflammation *(51, 52)*, both transcription factors contributed to the *HpbE*-triggered induction of type-2-suppressive mediators (PGE_2, IL-10 and IL-1β). In addition, p38 MAPK, which mediated the induction of COX metabolites, had previously been implicated in the modulation of macrophage activation by a protein from a filarial nematode (AvCystatin) *(53)*. However, if and how *Hpb* GDH may be involved in the activation of p38 MAPK-, NF-κB- or HIF-1α pathways, remains to be studied.

Last, as eicosanoids represent important mediators in severe and therapy-resistant type-2 inflammatory diseases *(5, 42, 54)*, their broad anti-inflammatory modulation by *HpbE* may represent a promising future therapeutic approach. The identification of *Hpb* GDH as a major eicosanoid-modulatory component of *HpbE* provides a basis for the development of a new helminth-based therapeutic enzyme with a unique immune regulatory profile.

Materials and Methods

Study design

The aim of this study was to investigate if and how helminth products could modulate eicosanoid pathways to regulate type-2 inflammation. We characterized eicosanoid profiles of multiple myeloid cell types after treatment with helminth preparations by LC-MS/MS and selected the most promising candidates (*HpbE* and its active component *Hpb GDH*) for *in vivo* and *ex vivo* testing. To define *in vivo* effects of *HpbE*, *Hpb GDH* or *HpbE*-conditioned macrophages, we treated mice intranasally with *HpbE* or recombinant *Hpb GDH* or transferred *HpbE*-conditioned macrophages during experimental HDM allergy and assessed type-2 inflammation by differential cell counts, histology and multiplex cytokine analysis. All read-outs were performed by a blinded experimenter. For the human part of our study, healthy volunteers (total n=15) and Aspirin-exacerbated respiratory disease (AERD) patients (n=6) (Caucasian men and women) were recruited. Sample sizes, replicates, and statistical methods are specified in the figure legends.

Mice

C57BL/6J mice were bred and maintained under specific pathogen free conditions at the École Polytechnique Fédérale de Lausanne (EPFL) or at the Centre Hospitalier Universitaire Vaudois (CHUV). Alternatively, BALB/c and C57BL/6J mice were obtained from Charles River Laboratories (Sulzfeld, Germany). Unless stated otherwise, 6-12 weeks old mice of both sexes were used. All animal experiments were approved by the local authorities (Swiss Veterinary Office or Regierung von Oberbayern).

Heligmosomoides polygyrus bakeri infection and preparation of larval extract

Infective stage-three larvae (L3) of *Heligmosomoides polygyrus bakeri* (*Hpb*) were obtained from the eggs of *Hpb*-infected mice as previously published *(55)*. For preparation of *Hpb* larval extract (*HpbE*), L3 larvae were homogenized in two cycles at 6.000 rpm for 60 seconds in a Precellys homogenizer using Precellys tough micro-organism lysing kits VK05 (Bertin Pharma). Remaining debris were removed by centrifugation (20 min, 14.000 rpm, 4°C). When indicated, heat inactivated-*HpbE (HpbE 90ºC)* was prepared by heating at 90ºC overnight.

House dust mite-induced allergic airway inflammation and intranasal treatment with *HpbE* or *Hpb* GDH

Eight weeks old female C57BL/6J mice were sensitized on day 0 by bilateral intranasal (i.n.) instillations of HDM extract from *Dermatophagoides farinae* (1 µg extract in 20 µl PBS; Stallergenes SA) and challenged on days 8-11 with 10 µg of the same extract dissolved in 20 µl PBS. Control animals received the same amount of PBS. *HpbE* treatment (5 µg *Hpb* extract in 20 µl PBS) was performed i.n. before sensitization and challenges, and *Hpb* GDH treatment (10 µg

protein in 20 µL PBS) i.n. before challenges. In the absence of *HpbE* or *Hpb* GDH treatment, the mice received 20 µl PBS. Three days after the last challenge, the airways of the mice were lavaged five times with 0.8 ml PBS. Aliquots of cell-free BAL fluid were frozen immediately with or without equal volumes of methanol. Viability, yield and differential cell count of BAL cells were performed as described before *(56)*.

Human blood and tissue samples

Peripheral blood mononuclear cells (PBMCs) or polymorphonuclear leukocytes (PMN) were isolated from the blood of healthy human donors or patients with Aspirin-exacerbated respiratory disease (AERD). Nasal polyp tissues were obtained during polypectomy of patients suffering from chronic rhinosinusitis with nasal polyps. Nasal polyp secretions were obtained from cultured nasal polyp tissues as described previously *(6)*. All blood and tissue donors participated in the study after informed written consent. Blood and tissue sampling and experiments including human blood cells were approved by the local ethics committee at the University clinic of the Technical University of Munich (internal reference: 422/16).

Macrophage cultures

Monocyte-derived macrophages (MDM) or bone marrow derived macrophages (BMDM) were generated by culture in the presence of human or murine recombinant GM-CSF (10 ng/ml) (Miltenyi Biotech) and human recombinant TGF-β1 (2 ng/ml) (Peprotech) as previously described *(6, 57)*. On day 6, cells were harvested and used for further experiments. More detailed procedures can be found in the Supplement.

Eicosanoid and cytokine analysis

Eicosanoids were quantified by liquid chromatography tandem mass spectrometry (LC-MS/MS) similar to a previously published method *(47)*. Cytokines were quantified using commercially available multiplex assays or ELISA kits according to the manufacturer's instructions. More detailed procedures can be found in the Supplement.

Chemotaxis assays

PMN were resuspended to a concentration of $1x10^6$ cells/ml in the presence of 100 ng/ml human GM-CSF (Miltenyi Biotech) and overnight stimulated with 10 μg/ml *HpbE*. When mentioned, PMN were pre-treated with 1 μM fluticasone propionate (Sigma-Aldrich), 10 μM montelukast (Cayman Chemical) or conditioned media from MDM stimulated overnight with 10 μg/ml *Hpb* extract +/- 100 μM Indomethacin for 1 hour. Nasal polyp secretions or a chemokine cocktail (2 ng/ml RANTES, 20 ng/ml IL-8 (Miltenyi Biotech) and 2 ng/ml LTB_4 (Cayman Chemical)) were placed in the lower wells of a chemotaxis plate (3 μm pore size; Corning). After mounting the transwell unit, $2x10^5$ PMN were added to the top of each well and migration was allowed for 3 hours at 37°C, 5% CO_2. The number of cells migrating to the lower well was counted microscopically. In some experiments, manual counting was validated by flow cytometry.

Statistical analysis

All statistical analysis for biological data was performed using GraphPad Prism (GraphPad Software Inc). Where two groups were compared, statistical significance was determined by Wilcoxon-Mann-Whitney test. Where more than two groups were compared, Kruskal-Wallis

followed by Dunn's multiple comparisons test, Friedman test (paired samples) or 2way ANOVA (unpaired samples) were used. Heat maps were generated using MetaboAnalyst version 3.0 (Mc Gill University), a free online tool for metabolomics data analysis.

Supplementary Materials

Supplementary materials and methods

Fig. S1. Heat map and volcano plot of PUFA metabolites produced by human MDM +/- treatment with *HpbE* and impact of *HpbE*-treated *Ptgs2*$^{-/-}$ BMDM on eosinophilic airway inflammation.

Fig. S2. *HpbE* has stronger eicosanoid-modulatory effects as compared to glucocorticosteroids.

Fig. S3. *HpbE* has a unique potential to induce type-2 suppressive mediators compared to other helminth products or helminth-associated bacteria.

Fig. S4. Viability and LTA4H expression in human eosinophils and neutrophils and heat map of PUFA metabolites produced by human PMN in response to treatment with *HpbE*.

Fig. S5. *HpbE* induces a regulatory eicosanoid- and cytokine profile in mixed and isolated CD14^{+} human PBMCs.

Fig. S6. Effect of COX-2-, NFκb-, PI3K-, PTEN- or PKA- inhibition on *HpbE*-driven modulation of cytokines and eicosanoid pathways.

Fig. S7. Effect of neutralizing antibodies against PRRs (TLR2 and dectins-1 and -2) or IL-1β on *HpbE*-driven modulation of eicosanoids and IL-10.

Fig. S8. Bithionol partially inhibits GDH activity, but does not affect cell viability and L3 stage *HpbE* shows a higher GDH activity as compared to L4 or L5 extracts.

Fig. S9. Newly generated monoclonal antibodies recognize *Hpb* GDH and clone 4F8, but not an isotype control antibody reduces *HpbE*-induced PGE_2 and IL-10 production.

Fig. S10. Sequence of *Hpb* GDH is distinct from human GDH and contains potential predicted glycosylation sites.

Table S1. LC-MS/MS panel of PUFAs and PUFA metabolites

Table S2. Proteins present in active fractions of *HpbE* identified by mass spectrometry

Table S3. Primer sequences for qPCR.

Table S4. Reagents and resources.

Data file S1. Primary data.

References *(58–62)*

References and Notes:

1. A. Ray, M. Raundhal, T. B. Oriss, P. Ray, S. E. Wenzel, Current concepts of severe asthma, *J. Clin. Invest.* **126**, 2394–2403 (2016).

2. A. A. White, D. D. Stevenson, Aspirin-Exacerbated Respiratory Disease, *N. Engl. J. Med.* **379**, 1060–1070 (2018).

3. M. C. Peters, S. Kerr, E. M. Dunican, P. G. Woodruff, M. L. Fajt, B. D. Levy, E. Israel, B. R. Phillips, D. T. Mauger, S. A. Comhair, S. C. Erzurum, M. W. Johansson, N. N. Jarjour, A. M. Coverstone, M. Castro, A. T. Hastie, E. R. Bleecker, S. E. Wenzel, J. V. Fahy, National Heart, Lung and Blood Institute Severe Asthma Research Program 3, Refractory airway type 2 inflammation in a large subgroup of asthmatic patients treated with inhaled corticosteroids, *J. Allergy Clin. Immunol.* **143**, 104-113.e14 (2019).

4. M. Takemura, A. Niimi, H. Matsumoto, T. Ueda, M. Yamaguchi, H. Matsuoka, M. Jinnai, K. F. Chung, M. Mishima, Imbalance of endogenous prostanoids in moderate-to-severe asthma, *Allergol Int* **66**, 83–88 (2017).

5. T. M. Laidlaw, J. A. Boyce, Aspirin-Exacerbated Respiratory Disease--New Prime Suspects, *N. Engl. J. Med.* **374**, 484–488 (2016).

6. K. Dietz, M. de Los Reyes Jiménez, E. S. Gollwitzer, A. M. Chaker, U. M. Zissler, O. P. Rådmark, H. A. Baarsma, M. Königshoff, C. B. Schmidt-Weber, B. J. Marsland, J. Esser-von Bieren, Age dictates a steroid-resistant cascade of Wnt5a, transglutaminase 2, and leukotrienes in inflamed airways, *J. Allergy Clin. Immunol.* (2016), doi:10.1016/j.jaci.2016.07.014.

7. L. Van Gerven, C. Langdon, A. Cordero, S. Cardelús, J. Mullol, I. Alobid, Lack of long-term add-on effect by montelukast in postoperative chronic rhinosinusitis patients with nasal polyps, *Laryngoscope* **128**, 1743–1751 (2018).

8. N. A. Barrett, O. M. Rahman, J. M. Fernandez, M. W. Parsons, W. Xing, K. F. Austen, Y. Kanaoka, Dectin-2 mediates Th2 immunity through the generation of cysteinyl leukotrienes, *J. Exp. Med* **208**, 593–604 (2011).

9. L. G. Bankova, D. F. Dwyer, E. Yoshimoto, S. Ualiyeva, J. W. McGinty, H. Raff, J. von Moltke, Y. Kanaoka, K. Frank Austen, N. A. Barrett, The cysteinyl leukotriene 3 receptor regulates expansion of IL-25-producing airway brush cells leading to type 2 inflammation, *Sci Immunol* **3** (2018), doi:10.1126/sciimmunol.aat9453.

10. E. D. Tait Wojno, L. A. Monticelli, S. V. Tran, T. Alenghat, L. C. Osborne, J. J. Thome, C. Willis, A. Budelsky, D. L. Farber, D. Artis, The prostaglandin D2 receptor CRTH2 regulates accumulation of group 2 innate lymphoid cells in the inflamed lung, *Mucosal Immunol* (2015), doi:10.1038/mi.2015.21.

11. Z. Zasłona, K. Okunishi, E. Bourdonnay, R. Domingo-Gonzalez, B. B. Moore, N. W. Lukacs, D. M. Aronoff, M. Peters-Golden, Prostaglandin E_2 suppresses allergic sensitization and lung inflammation by targeting the E prostanoid 2 receptor on T cells, *J. Allergy Clin. Immunol.* **133**, 379–387 (2014).

12. C. Draijer, C. E. Boorsma, C. Reker-Smit, E. Post, K. Poelstra, B. N. Melgert, PGE2-treated macrophages inhibit development of allergic lung inflammation in mice, *J. Leukoc. Biol.* **100**, 95–102 (2016).

13. W. Zhou, K. Goleniewska, J. Zhang, D. E. Dulek, S. Toki, M. T. Lotz, D. C. Newcomb, M. G. Boswell, V. V. Polosukhin, G. L. Milne, P. Wu, M. L. Moore, G. A. FitzGerald, R. S. Peebles, Cyclooxygenase inhibition abrogates aeroallergen-induced immune tolerance by suppressing prostaglandin I2 receptor signaling, *J. Allergy Clin. Immunol.* (2014), doi:10.1016/j.jaci.2014.06.004.

14. J. Säfholm, M. L. Manson, J. Bood, I. Delin, A.-C. Orre, P. Bergman, M. Al-Ameri, S.-E. Dahlén, M. Adner, Prostaglandin E2 inhibits mast cell-dependent bronchoconstriction in human small airways through the E prostanoid subtype 2 receptor, *J. Allergy Clin. Immunol.* **136**, 1232-1239.e1 (2015).

15. M. M. M. Kaisar, M. Ritter, C. Del Fresno, H. S. Jónasdóttir, A. J. van der Ham, L. R. Pelgrom, G. Schramm, L. E. Layland, D. Sancho, C. Prazeres da Costa, M. Giera, M. Yazdanbakhsh, B. Everts, Dectin-1/2-induced autocrine PGE2 signaling licenses dendritic cells to prime Th2 responses, *PLoS Biol.* **16**, e2005504 (2018).

16. M. L. Patnode, J. K. Bando, M. F. Krummel, R. M. Locksley, S. D. Rosen, Leukotriene B4 amplifies eosinophil accumulation in response to nematodes, *J. Exp. Med.* **211**, 1281–1288 (2014).

17. T. A. Wynn, Type 2 cytokines: mechanisms and therapeutic strategies, *Nat. Rev. Immunol.* **15**, 271–282 (2015).

18. J. R. Grainger, K. A. Smith, J. P. Hewitson, H. J. McSorley, Y. Harcus, K. J. Filbey, C. A. M. Finney, E. J. D. Greenwood, D. P. Knox, M. S. Wilson, Y. Belkaid, A. Y. Rudensky, R. M. Maizels, Helminth secretions induce de novo T cell Foxp3 expression and regulatory function through the TGF-β pathway, *J. Exp. Med.* **207**, 2331–2341 (2010).

19. S. Navarro, D. A. Pickering, I. B. Ferreira, L. Jones, S. Ryan, S. Troy, A. Leech, P. J. Hotez, B. Zhan, T. Laha, R. Prentice, T. Sparwasser, J. Croese, C. R. Engwerda, J. W. Upham, V. Julia, P. R. Giacomin, A. Loukas, Hookworm recombinant protein promotes regulatory T cell responses that suppress experimental asthma, *Sci Transl Med* **8**, 362ra143 (2016).

20. M. Osbourn, D. C. Soares, F. Vacca, E. S. Cohen, I. C. Scott, W. F. Gregory, D. J. Smyth, M. Toivakka, A. M. Kemter, T. le Bihan, M. Wear, D. Hoving, K. J. Filbey, J. P. Hewitson, H. Henderson, A. Gonzàlez-Cìscar, C. Errington, S. Vermeren, A. L. Astier, W. A. Wallace, J. Schwarze, A. C. Ivens, R. M. Maizels, H. J. McSorley, HpARI Protein Secreted by a Helminth Parasite Suppresses Interleukin-33, *Immunity* **47**, 739-751.e5 (2017).

21. H. J. McSorley, N. F. Blair, K. A. Smith, A. N. J. McKenzie, R. M. Maizels, Blockade of IL-33 release and suppression of type 2 innate lymphoid cell responses by helminth secreted products in airway allergy, *Mucosal Immunol* **7**, 1068–1078 (2014).

22. M. M. Zaiss, K. M. Maslowski, I. Mosconi, N. Guenat, B. J. Marsland, N. L. Harris, IL-1β suppresses innate IL-25 and IL-33 production and maintains helminth chronicity, *PLoS Pathog.* **9**, e1003531 (2013).

23. R. M. Maizels, H. H. Smits, H. J. McSorley, Modulation of Host Immunity by Helminths: The Expanding Repertoire of Parasite Effector Molecules, *Immunity* **49**, 801–818 (2018).

24. D. L. Clarke, N. H. E. Davis, C. L. Campion, M. L. Foster, S. C. Heasman, A. R. Lewis, I. K. Anderson, D. J. Corkill, M. A. Sleeman, R. D. May, M. J. Robinson, Dectin-2 sensing of house dust mite is critical for the initiation of airway inflammation, *Mucosal Immunol* **7**, 558–567 (2014).

25. T. Liu, T. M. Laidlaw, C. Feng, W. Xing, S. Shen, G. L. Milne, J. A. Boyce, Prostaglandin E2 deficiency uncovers a dominant role for thromboxane A2 in house dust mite-induced allergic pulmonary inflammation, *Proc. Natl. Acad. Sci. U.S.A.* **109**, 12692–12697 (2012).

26. Z. Zasłona, S. Przybranowski, C. Wilke, N. van Rooijen, S. Teitz-Tennenbaum, J. J. Osterholzer, J. E. Wilkinson, B. B. Moore, M. Peters-Golden, Resident alveolar macrophages suppress, whereas recruited monocytes promote, allergic lung inflammation in murine models of asthma, *J. Immunol.* **193**, 4245–4253 (2014).

27. L. Guo, G. Wei, J. Zhu, W. Liao, W. J. Leonard, K. Zhao, W. Paul, IL-1 family members and STAT activators induce cytokine production by Th2, Th17, and Th1 cells, *Proc. Natl. Acad. Sci. U.S.A.* **106**, 13463–13468 (2009).

28. F. Kratochvill, G. Neale, J. M. Haverkamp, L.-A. Van de Velde, A. M. Smith, D. Kawauchi, J. McEvoy, M. F. Roussel, M. A. Dyer, J. E. Qualls, P. J. Murray, TNF Counterbalances the Emergence of M2 Tumor Macrophages, *Cell Rep* **12**, 1902–1914 (2015).

29. S. A. Mathie, K. L. Dixon, S. A. Walker, V. Tyrrell, M. Mondhe, V. B. O'Donnell, L. G. Gregory, C. M. Lloyd, Alveolar macrophages are sentinels of murine pulmonary homeostasis following inhaled antigen challenge, *Allergy* **70**, 80–89 (2015).

30. H. Qin, A. T. Holdbrooks, Y. Liu, S. L. Reynolds, L. L. Yanagisawa, E. N. Benveniste, SOCS3 deficiency promotes M1 macrophage polarization and inflammation, *J. Immunol.* **189**, 3439–3448 (2012).

31. C. Schnoeller, S. Rausch, S. Pillai, A. Avagyan, B. M. Wittig, C. Loddenkemper, A. Hamann, E. Hamelmann, R. Lucius, S. Hartmann, A helminth immunomodulator reduces allergic and inflammatory responses by induction of IL-10-producing macrophages, *J. Immunol.* **180**, 4265–4272 (2008).

32. F. O. Martinez, L. Helming, R. Milde, A. Varin, B. N. Melgert, C. Draijer, B. Thomas, M. Fabbri, A. Crawshaw, L. P. Ho, N. H. Ten Hacken, V. Cobos Jiménez, N. A. Kootstra, J. Hamann, D. R. Greaves, M. Locati, A. Mantovani, S. Gordon, Genetic programs expressed in resting and IL-4 alternatively activated mouse and human macrophages: similarities and differences, *Blood* **121**, e57-69 (2013).

33. K. E. Fujimura, A. R. Sitarik, S. Havstad, D. L. Lin, S. Levan, D. Fadrosh, A. R. Panzer, B. LaMere, E. Rackaityte, N. W. Lukacs, G. Wegienka, H. A. Boushey, D. R. Ownby, E. M. Zoratti, A. M. Levin, C. C. Johnson, S. V. Lynch, Neonatal gut microbiota associates with childhood multisensitized atopy and T cell differentiation, *Nat. Med.* **22**, 1187–1191 (2016).

34. M. S. Wilson, M. D. Taylor, A. Balic, C. A. M. Finney, J. R. Lamb, R. M. Maizels, Suppression of allergic airway inflammation by helminth-induced regulatory T cells, *J. Exp. Med.* **202**, 1199–1212 (2005).

35. K. Ramaswamy, P. Kumar, Y. X. He, A role for parasite-induced PGE2 in IL-10-mediated host immunoregulation by skin stage schistosomula of Schistosoma mansoni, *J. Immunol.* **165**, 4567–4574 (2000).

36. M. M. Zaiss, A. Rapin, L. Lebon, L. K. Dubey, I. Mosconi, K. Sarter, A. Piersigilli, L. Menin, A. W. Walker, J. Rougemont, O. Paerewijck, P. Geldhof, K. D. McCoy, A. J. Macpherson, J. Croese, P. R. Giacomin, A. Loukas, T. Junt, B. J. Marsland, N. L. Harris, The Intestinal Microbiota Contributes to the Ability of Helminths to Modulate Allergic Inflammation, *Immunity* **43**, 998–1010 (2015).

37. K. Pal, X. Feng, J. W. Steinke, M. D. Burdick, Y. M. Shim, S.-S. Sung, W. G. Teague, L. Borish, Leukotriene A4 Hydrolase Activation and Leukotriene B4 Production by Eosinophils in Severe Asthma, *Am. J. Respir. Cell Mol. Biol.* **60**, 413–419 (2019).

38. B. D. Levy, C. B. Clish, B. Schmidt, K. Gronert, C. N. Serhan, Lipid mediator class switching during acute inflammation: signals in resolution, *Nat. Immunol.* **2**, 612–619 (2001).

39. N. Scheerer, N. Dehne, C. Stockmann, S. Swoboda, H. A. Baba, A. Neugebauer, R. S. Johnson, J. Fandrey, Myeloid hypoxia-inducible factor-1α is essential for skeletal muscle regeneration in mice, *J. Immunol.* **191**, 407–414 (2013).

40. M. K. Cho, M. K. Park, S. A. Kang, S. K. Park, J. H. Lyu, D.-H. Kim, H.-K. Park, H. S. Yu, TLR2-dependent amelioration of allergic airway inflammation by parasitic nematode type II MIF in mice, *Parasite Immunol.* **37**, 180–191 (2015).

41. M. Ritter, O. Gross, S. Kays, J. Ruland, F. Nimmerjahn, S. Saijo, J. Tschopp, L. E. Layland, C. Prazeres da Costa, Schistosoma mansoni triggers Dectin-2, which activates the Nlrp3 inflammasome and alters adaptive immune responses, *Proc. Natl. Acad. Sci. U.S.A.* **107**, 20459–20464 (2010).

42. S. K. Samuchiwal, J. A. Boyce, Role of lipid mediators and control of lymphocyte responses in type 2 immunopathology, *J. Allergy Clin. Immunol.* **141**, 1182–1190 (2018).

43. L. van de Laar, W. Saelens, S. De Prijck, L. Martens, C. L. Scott, G. Van Isterdael, E. Hoffmann, R. Beyaert, Y. Saeys, B. N. Lambrecht, M. Guilliams, Yolk Sac Macrophages, Fetal Liver, and Adult Monocytes Can Colonize an Empty Niche and Develop into Functional Tissue-Resident Macrophages, *Immunity* **44**, 755–768 (2016).

44. X. Yu, A. Buttgereit, I. Lelios, S. G. Utz, D. Cansever, B. Becher, M. Greter, The Cytokine TGF-β Promotes the Development and Homeostasis of Alveolar Macrophages, *Immunity* **47**, 903-912.e4 (2017).

45. J. Maric, A. Ravindran, L. Mazzurana, Å. K. Björklund, A. Van Acker, A. Rao, D. Friberg, S.-E. Dahlén, A. Heinemann, V. Konya, J. Mjösberg, PGE2 suppresses human group 2 innate lymphoid cell function, *J. Allergy Clin. Immunol.* (2017), doi:10.1016/j.jaci.2017.09.050.

46. W. Zhou, S. Toki, J. Zhang, K. Goleniewksa, D. C. Newcomb, J. Y. Cephus, D. E. Dulek, M. H. Bloodworth, M. T. Stier, V. Polosuhkin, R. D. Gangula, S. A. Mallal, D. H. Broide, R. S. Peebles, Prostaglandin I2 Signaling and Inhibition of Group 2 Innate Lymphoid Cell Responses, *Am. J. Respir. Crit. Care Med.* **193**, 31–42 (2016).

47. F. D. R. Henkel, A. Friedl, M. Haid, D. Thomas, T. Bouchery, P. Haimerl, M. de Los Reyes Jiménez, F. Alessandrini, C. B. Schmidt-Weber, N. L. Harris, J. Adamski, J. Esser-von Bieren, House dust mite drives proinflammatory eicosanoid reprogramming and macrophage effector functions, *Allergy* (2018), doi:10.1111/all.13700.

48. C. C. Kao, A. D. Parulekar, Spotlight on fevipiprant and its potential in the treatment of asthma: evidence to date, *J Asthma Allergy* **12**, 1–5 (2019).

49. H. J. McSorley, M. T. O'Gorman, N. Blair, T. E. Sutherland, K. J. Filbey, R. M. Maizels, Suppression of type 2 immunity and allergic airway inflammation by secreted products of the helminth Heligmosomoides polygyrus, *European journal of immunology* (2012), doi:10.1002/eji.201142161.

50. C. J. C. Johnston, D. J. Smyth, R. B. Kodali, M. P. J. White, Y. Harcus, K. J. Filbey, J. P. Hewitson, C. S. Hinck, A. Ivens, A. M. Kemter, A. O. Kildemoes, T. Le Bihan, D. C. Soares, S. M. Anderton, T. Brenn, S. J. Wigmore, H. V. Woodcock, R. C. Chambers, A. P. Hinck, H. J. McSorley, R. M. Maizels, A structurally distinct TGF-β mimic from an intestinal helminth parasite potently induces regulatory T cells, *Nat Commun* **8**, 1741 (2017).

51. W. Han, M. Joo, M. B. Everhart, J. W. Christman, F. E. Yull, T. S. Blackwell, Myeloid cells control termination of lung inflammation through the NF-κB pathway, *Am J Physiol Lung Cell Mol Physiol* **296**, L320–L327 (2009).

52. M. Toussaint, L. Fievez, P.-V. Drion, D. Cataldo, F. Bureau, P. Lekeux, C. J. Desmet, Myeloid hypoxia-inducible factor 1α prevents airway allergy in mice through macrophage-mediated immunoregulation, *Mucosal Immunol* **6**, 485–497 (2013).

53. C. Klotz, T. Ziegler, A. S. Figueiredo, S. Rausch, M. R. Hepworth, N. Obsivac, C. Sers, R. Lang, P. Hammerstein, R. Lucius, S. Hartmann, A helminth immunomodulator exploits host signaling events to regulate cytokine production in macrophages, *PLoS Pathog.* **7**, e1001248 (2011).

54. B. Hilvering, T. S. C. Hinks, L. Stöger, E. Marchi, M. Salimi, R. Shrimanker, W. Liu, W. Chen, J. Luo, S. Go, T. Powell, J. Cane, S. Thulborn, A. Kurioka, T. Leng, J. Matthews, C. Connolly, C. Borg, M. Bafadhel, C. B. Willberg, A. Ramasamy, R. Djukanović, G. Ogg, I. D. Pavord, P. Klenerman, L. Xue, Synergistic activation of pro-inflammatory type-2 CD8+ T lymphocytes by lipid mediators in severe eosinophilic asthma, *Mucosal Immunol* **11**, 1408–1419 (2018).

55. M. Camberis, G. Le Gros, J. Urban Jr, Animal model of Nippostrongylus brasiliensis and Heligmosomoides polygyrus, *Curr Protoc Immunol* **Chapter 19**, Unit 19.12 (2003).

56. F. Alessandrini, H. Schulz, S. Takenaka, B. Lentner, E. Karg, H. Behrendt, T. Jakob, Effects of ultrafine carbon particle inhalation on allergic inflammation of the lung, *J. Allergy Clin. Immunol.* **117**, 824–830 (2006).

57. J. Esser-von Bieren, I. Mosconi, R. Guiet, A. Piersgilli, B. Volpe, F. Chen, W. C. Gause, A. Seitz, J. S. Verbeek, N. L. Harris, Antibodies Trap Tissue Migrating Helminth Larvae and Prevent Tissue Damage by Driving IL-4Rα-Independent Alternative Differentiation of Macrophages, *PLoS Pathog.* **9**, e1003771 (2013).

58. A. Bepperling, F. Alte, T. Kriehuber, N. Braun, S. Weinkauf, M. Groll, M. Haslbeck, J. Buchner, Alternative bacterial two-component small heat shock protein systems, *Proc. Natl. Acad. Sci. U.S.A.* **109**, 20407–20412 (2012).

59. E. V. Mymrikov, M. Daake, B. Richter, M. Haslbeck, J. Buchner, The Chaperone Activity and Substrate Spectrum of Human Small Heat Shock Proteins, *J. Biol. Chem.* **292**, 672–684 (2017).

60. Y. Zhang, U. Werling, W. Edelmann, Seamless Ligation Cloning Extract (SLiCE) Cloning Method, *Methods Mol Biol* **1116**, 235–244 (2014).

61. A. de Marco, Protocol for preparing proteins with improved solubility by co-expressing with molecular chaperones in Escherichia coli, *Nat Protoc* **2**, 2632–2639 (2007).

62. F. W. Studier, Protein production by auto-induction in high density shaking cultures, *Protein Expr. Purif.* **41**, 207–234 (2005).

References 58-62: Supplement

Acknowledgments: The authors wish to thank Dr. Mark Haid and Prof. Dr. Jerzy Adamski (Helmholtz Center Munich) for support with LC-MS/MS analysis. The authors also wish to

thank the animal caretakers of the University of Lausanne and Helmholtz Center Munich for animal husbandry. The authors further gratefully acknowledge technical assistance by Manuel Kulagin, Julia Steinmetz, Dr. Marina Korotkova, Dr. Nathalie Dehne, Dr. Felix Lauffer, Dr. Maximilian Schiener and Johanna Grösch. We also wish to thank staff of the monoclonal antibody facility at the Helmholtz Center Munich (Dr. Regina Federle, Dr. Aloys Schepers, Andrew Flatley) for generating and providing *Hpb* GDH specific monoclonal antibodies.

Funding: This study was supported by the German Research Foundation (DFG) with grants ES 471/2-1 and FOR 2599_A07 (ES 471/3-1), by the Else Kröner-Fresenius-Stiftung (grant 2015_A195), by the Fritz Thyssen Foundation (Az. 10.17.2.017MN) and a Helmholtz Young Investigator grant (VH-NG-1331) to J.E.v.B;

Author contributions: Conceptualization, J.E.v.B., C.B.S.W.; Methodology, M.R.J, A.L., F.A., D.T., B.B., R.N., M.H., P.J.J., D.V., M.F., A.G., A.M., N.L.H., B.J.M., J.E.v.B.; Investigation, M.R.J, A.L., F.A., S.S., P.H., F.H., W.A.N., A.T., C.P.C., A.M.C., M.H., C.O., J.E.v.B.; Writing: M.R.J., A.L. and J.E.v.B; Funding acquisition: J.E.v.B;

Competing interests: J.E.v.B. and C.B.S.W have submitted a patent application related to the immune regulatory effects of *HpbE* and its components. C.B.S.W received grant support from Allergopharma, PLS Design as well as Zeller AG and received speaker honoraria from Allergopharma. A.M.C reports to have given lectures sponsored by Allergopharma, ALK, GSK and received grant support or consultant arrangements via Technische Universität München with Allergopharma, ALK, HAL-Allergy, Mundipharma, Lofarma, Zeller AG, Novartis.

Figure legends

Fig. 1. Topical treatment with *Hpb* larval extract (*HpbE*) modulates type-2 inflammation.

(**A**) Experimental model of house dust mite (HDM)-induced allergic airway inflammation and intranasal (i.n) treatment with *HpbE;* (**B**), BALF cell counts in mice sensitized and challenged with HDM (1 μg/ 10 μg) ± i.n. treatment with *HpbE* (5 μg), 48h after the last challenge and treatment. (**C**) Representative hematoxylin and eosin (H&E)- or Periodic acid-Schiff (PAS) stained lung tissue from mice sensitized to HDM ± treatment with *HpbE*. Scale bar: 100 μm. (**D**) Levels of 15-HETE (LC-MS/MS) or IL-5, IL-6, eotaxin and RANTES (Bioplex) in BALF from mice sensitized to HDM ± treatment with *HpbE*. Results are pooled from two independent experiments (B, D) or representative of stainings performed for two independent experiments (C). Results are presented as mean ± SEM, n=3-9 (naïve) or n=5-17 (treated) per group. Statistical significance was determined by Kruskal-Wallis test followed by Dunn's multiple comparison test. *$p < 0.05$, **$p < 0.01$, ***$p<0.001$.

Fig. 2. *HpbE*-treated macrophages produce reduced levels of leukotrienes and modulate allergic airway inflammation via prostaglandin E_2.

(**A**) Eicosanoid levels (LC-MS/MS) produced by mouse bone marrow macrophages (BMDM) after treatment with *Hpb* larval extract (*HpbE*) (24h) and stimulation with A23187 (10 min). (**B**) Relative gene expression of AA-metabolizing enzymes (qPCR) in mouse BMDM treated with *HpbE*. (**C**) Heat map showing major PUFA metabolites (LC-MS/MS) produced by human monocyte-derived macrophages (MDM) ± treatment with *HpbE* followed by A23187 (10 min). (**D**) Levels of major bioactive AA metabolites (LC-MS/MS) produced by human MDM ± treatment with *HpbE* +A23187 (10 min). (**E**) Relative gene expression of eicosanoid pathway

proteins (qPCR) in human MDM ± treatment with *HpbE*. (**F**) Frequencies and total numbers of eosinophils in BALF of mice sensitized to HDM + i.n. transfer of *HpbE*-conditioned or untreated BMDM (MΦ) (wildtype (wt) or *Ptges*$^{-/-}$), 18h after the last challenge and transfer. Dashed lines indicate eosinophil levels in HDM-sensitized mice. (**G**) Representative H&E stained lung tissue from mice sensitized to HDM ± intranasal transfer of untreated or *HpbE*-conditioned BMDM (wt or *Ptges*$^{-/-}$). Scale bar: 100 μm. Data are presented as mean ± SEM, n=8 BMDM from C57BL/6 mice (A,B); n=10-15 MDM from healthy human blood donors (C-E); n=7-9 mice per group (F,G). Statistical significance was determined by Wilcoxon test (A-E) or Mann Whitney test (F). *p<0.05, **p<0.01, ***p<0.001.

Fig. 3. *HpbE* induces type-2-suppressive cytokines and prevents M2 polarization.

(**A**) Levels of IL-10 and IL-1β (ELISA) produced by human MDM ± treatment with *HpbE*. (**B**) Levels of TNF-α, IL-6, IL-12p70, IL-18, IL-27, IL-33 and CCL17/TARC (Bioplex) produced by human MDM after treatment with *HpbE*. (**C**) Levels of IL-10 and IL-1β (Bioplex) produced by mouse BMDM ± treatment with *HpbE*. (**D**) Gene expression of M2 markers (qPCR) in human MDM ± treatment with *HpbE*. (**E**) Gene expression of M2 markers (qPCR) in mouse BMDM ± treatment with *HpbE*. Data are presented as mean ± SEM, n=3-15 MDM from healthy human blood donors, n=5-8 BMDM from C57BL/6 mice. Statistical significance was determined by Wilcoxon test. *p<0.05, **p<0.01, ***p<0.001.

Fig. 4. *HpbE* modulates eicosanoid profiles and chemotaxis of granulocytes in a human setting of type-2 inflammation.

(**A**) Heat map showing major PUFA metabolites (LC-MS/MS) produced by mixed human granulocytes ± treatment with *HpbE* (24h) followed by A23187 (10 min). (**B**) Levels of major eicosanoids (LC-MS/MS) produced by mixed human granulocytes ± treatment with *HpbE* (24h) + A23187 (10 min). (**C**) Levels of cysLTs (EIA, validated by LC-MS/MS) produced by purified human eosinophils ± treatment with *HpbE* (24h) + A23187 (10 min). (**D**) Relative gene expression of AA-metabolizing enzymes (qPCR) in mixed human granulocytes ± treatment with *HpbE*. (**E**) Levels of LT-synthetic enzymes (LTC_4S and LTA_4H) (flow cytometry) in human eosinophils ± treatment with *HpbE*. (**F**) Chemotaxis of granulocytes from AERD patients towards nasal polyp secretions ± treatment with *HpbE* /fluticasone propionate / montelukast, MK. Dashed line depicts basal migration. (**G**) Levels of chemotactic receptors (CCR3 and CRTH2) (flow cytometry) in human eosinophils ± treatment with *HpbE*. (**H**) Chemotaxis of human granulocytes ± pre-treatment with conditioned media from MDM (± *HpbE,* ± COX-inhibitor indomethacin). Dashed line depicts basal migration. Data are pooled from at least 3 independent experiments and presented as mean ± SEM, n=6-9 mixed granulocytes or purified eosinophils from human blood donors. Statistical significance was determined by Wilcoxon test (two groups) or Friedman test (four groups), *$p<0.05$, **$p<0.01$.

Fig. 5. Induction of type-2-suppressive macrophages by *HpbE* is mediated via HIF-1α, p-38 MAPK and COX.

(**A**) Representative immunofluorescence staining of HIF-1α, COX-2, DAPI (cell nuclei) and F4/80 in BMDM ± treatment with *HpbE*. (**B**) Eicosanoid levels (LC-MS/MS) in BMDM (wt or HIF-$1\alpha^{floxed/floxed}$xLysMCre) ± treatment with *HpbE* (24h) + A23187 (10 min). (**C**) Levels of IL-6, TNFα, IL-1β or IL-10 (Bioplex) in BMDM (wt or HIF-$1\alpha^{floxed/floxed}$xLysMCre) ± treatment

with *HpbE*. (**D**) Gene expression of M2 markers (qPCR) in BMDM (wt or HIF-1α$^{floxed/floxed}$xLysMCre) ± treatment with *HpbE*. (**E**) Protein levels of phospho-p38, total p38, COX-2 or β-actin (westernblot) in MDM ± treatment with *HpbE*. Left: representative blots for n=3 blood donors; right: quantification for n=5-9 donors. (**F**, **G**) Levels of IL-10 or IL-1β (ELISA) in MDM ± treatment with *HpbE* ± inhibitors of p-38 (VX-702), COX (indomethacin) or HIF-1α (acriflavine). (**H**) Fold change of eicosanoid enzymes in MDM treated with *HpbE* ± inhibitors of p-38 (VX-702), COX (indomethacin) or HIF-1α (acriflavine). Dotted lines indicate levels in untreated cells. Data are pooled from at least 2 independent experiments and presented as mean ± SEM, n=5-9. Statistical significance was determined by 2way ANOVA (A-D), Wilcoxon test (E) or Friedman test (F-H). * $p<0.05$, ** $p<0.01$, ***$p<0.001$.

Figure 6: Glutamate dehydrogenase is a major immune regulatory protein in *HpbE.*

(**A**, **B**) Levels of prostanoids (EIA) or IL-10 and IL-1β (ELISA) in human MDM (A) or chemotaxis of human PMN (B) ± treatment with *HpbE* or heat-inactivated *HpbE* (*HpbE* 90°C) (**C**) Levels of IL-10 (ELISA) in MDM ± treatment with *HpbE* ± pretreatment with proteinase K (prot K). (**D**) Size exclusion chromatogram for fractionation of *HpbE*. (**E**) Levels of TXB_2 (EIA) or IL-10 (ELISA) in MDM ± treatment with *HpbE* fractions. (**F**) Summary of results from mass-spectrometric identification of proteins in active fractions of *HpbE*. (**G**) Levels of PGE_2 (EIA) or IL-10 (ELISA) in MDM ± treatment with *HpbE* ± inhibitor of GDH (GDHi, bithionol, 20 μM). (**H**) Levels of PGE_2 or total COX metabolites (LC-MS/MS) in MDM ± treatment with *HpbE* ± inhibitor of GDH (GDHi, bithionol, 20 μM or 100 μM). (**I**) Levels of PGE_2 (EIA) or IL-10 (ELISA) in MDM ± treatment with *HpbE* ± different dilutions of a monoclonal antibody (clone 4F8) against *Hpb* GDH. Data are pooled from at least 2 independent experiments and presented

as mean ± SEM for MDM from n=2-10 healthy human blood donors. Statistical significance was determined by Friedman test. *p<0.05, **p<0.01, ***p<0.001.

Figure 7: Recombinant *Hpb* GDH induces anti-inflammatory mediators in human macrophages and suppresses allergic airway inflammation in mice.

(**A**) Levels of eicosanoids (LC-MS/MS/ EIA) or IL-10 (ELISA) in human MDM ± treatment with recombinant *Hpb* GDH (5 µg/ml) (24h) ± A23187 (10 min). (**B**) BALF cell counts in mice sensitized and challenged with HDM (1 µg/ 10 µg) ± i.n. treatment with *Hpb* GDH (10 µg), 48h after the last challenge and treatment. (**C**) Representative hematoxylin and eosin (H&E)- or Periodic acid-Schiff (PAS) stained lung tissue from mice sensitized to HDM ± treatment with *HpbE*. Scale bar: 100 µm. Results are pooled from at least two independent experiments (A, B) or representative of stainings performed for two independent experiments (C). Results are presented as mean ± SEM, for MDM from n=7-9 healthy human blood donors or n=9-10 mice per group. Statistical significance was determined by Friedman test (A) or Kruskal-Wallis test followed by Dunn's multiple comparison test (B). *p = 0.05, **p = 0.01, ***p<0.001.

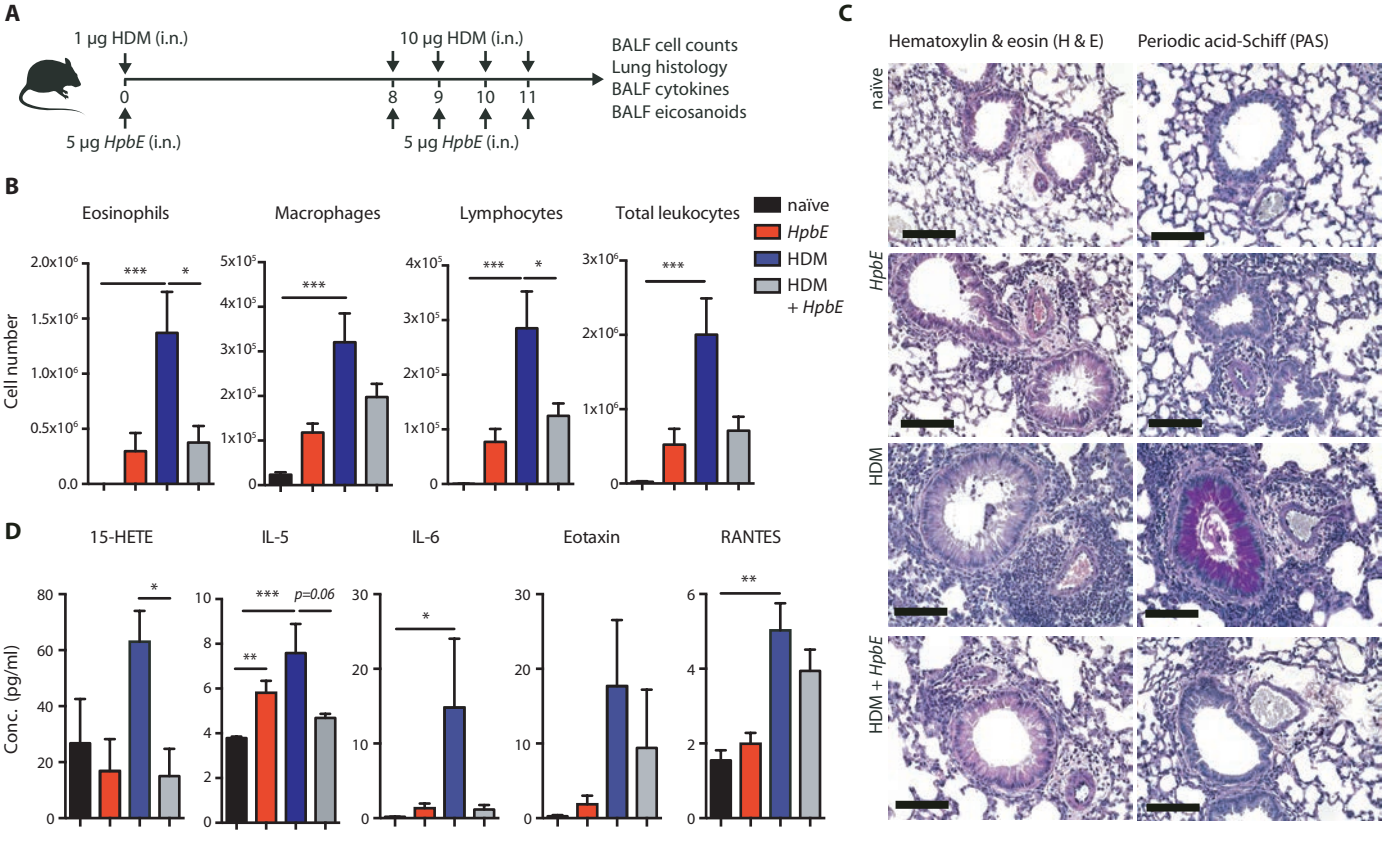
A
1 µg HDM (i.n.)
10 µg HDM (i.n.)
BALF cell counts
Lung histology
BALF cytokines
BALF eicosanoids
0
8
9
10
11
5 µg HpbE (i.n.)
5 µg HpbE (i.n.)
B
Eosinophils
Macrophages
Lymphocytes
Total leukocytes
naïve
HpbE
HDM
HDM + HpbE
Cell number
C
Hematoxylin & eosin (H & E)
Periodic acid-Schiff (PAS)
naïve
HpbE
HDM
HDM + HpbE
D
15-HETE
IL-5
IL-6
Eotaxin
RANTES
Conc. (pg/ml)
p=0.06

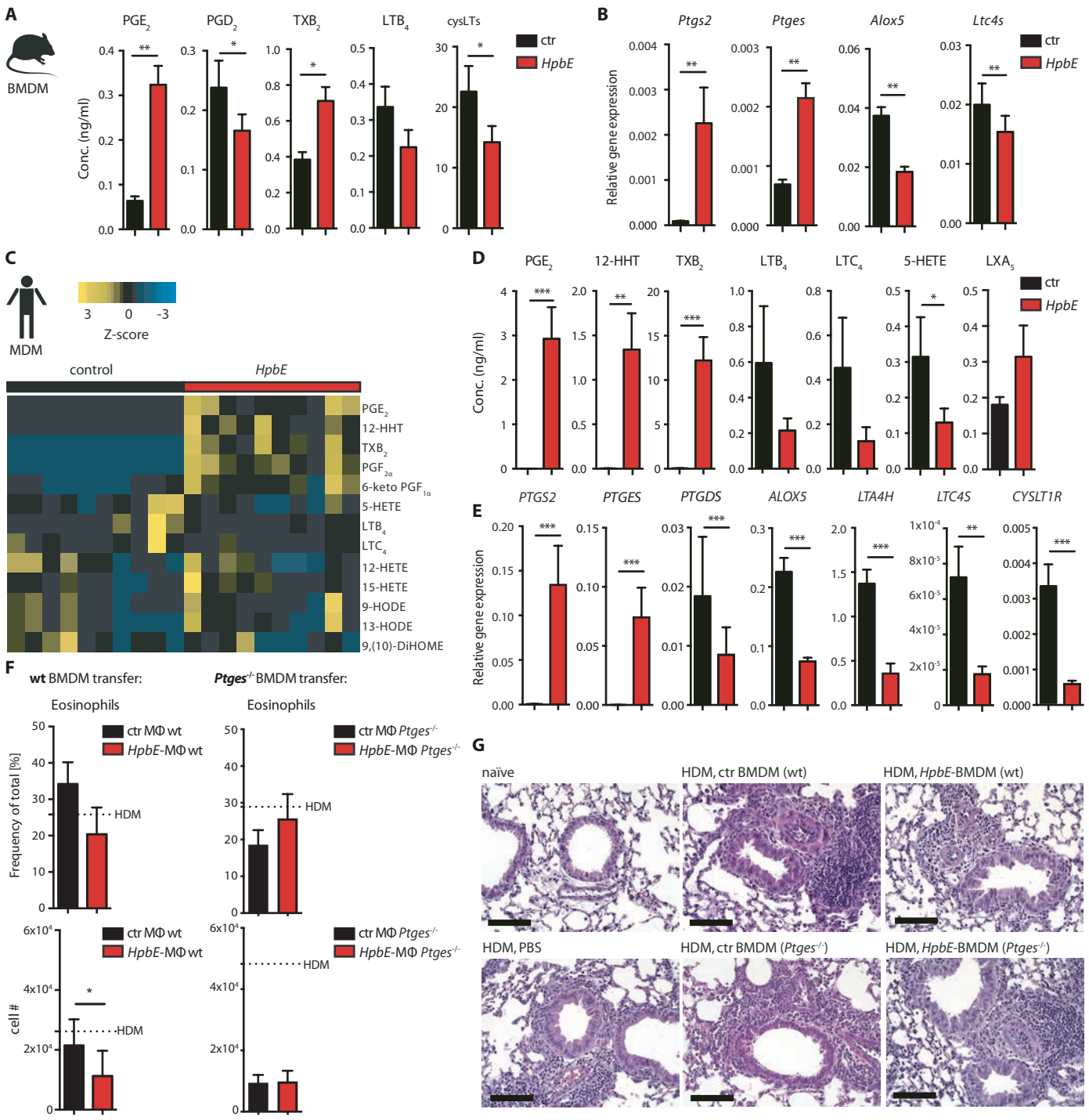
A
BMDM
PGE2
PGD2
TXB2
LTB4
cysLTs
Conc. (ng/ml)
ctr
HpbE
B
Ptgs2
Ptges
Alox5
Ltc4s
Relative gene expression
C
MDM
3
0
-3
Z-score
control
HpbE
PGE2
12-HHT
TXB2
PGF2α
6-keto PGF1α
5-HETE
LTB4
LTC4
12-HETE
15-HETE
9-HODE
13-HODE
9,(10)-DiHOME
D
PGE2
12-HHT
TXB2
LTB4
LTC4
5-HETE
LXA5
Conc. (ng/ml)
E
PTGS2
PTGES
PTGDS
ALOX5
LTA4H
LTC4S
CYSLT1R
Relative gene expression
F
wt BMDM transfer:
Ptges-/- BMDM transfer:
Eosinophils
ctr MΦ wt
HpbE-MΦ wt
ctr MΦ Ptges-/-
HpbE-MΦ Ptges-/-
HDM
Frequency of total [%]
cell #
G
naïve
HDM, ctr BMDM (wt)
HDM, HpbE-BMDM (wt)
HDM, PBS
HDM, ctr BMDM (Ptges-/-)
HDM, HpbE-BMDM (Ptges-/-)

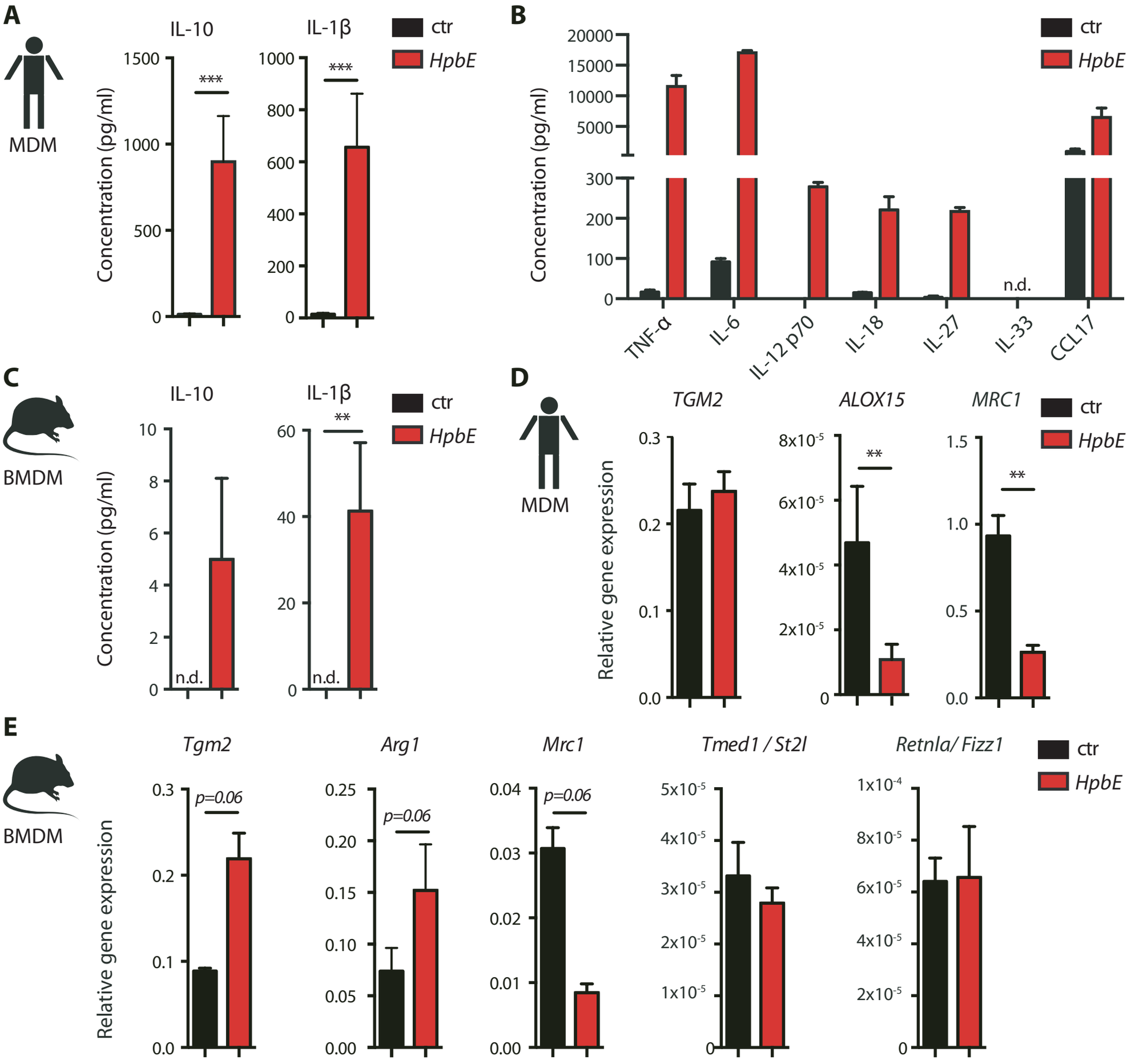
A
MDM
IL-10
IL-1β
ctr
HpbE
Concentration (pg/ml)
1500
1000
500
0
***
1000
800
600
400
200
0
***
B
Concentration (pg/ml)
20000
15000
10000
5000
300
200
100
0
n.d.
TNF-α
IL-6
IL-12 p70
IL-18
IL-27
IL-33
CCL17
C
BMDM
IL-10
IL-1β
ctr
HpbE
Concentration (pg/ml)
10
8
6
4
2
0
n.d.
60
40
20
0
**
n.d.
D
MDM
TGM2
ALOX15
MRC1
ctr
HpbE
Relative gene expression
0.3
0.2
0.1
0.0
8x10-5
6x10-5
4x10-5
2x10-5
0
**
1.5
1.0
0.5
0.0
**
E
BMDM
Tgm2
Arg1
Mrc1
Tmed1 / St2l
Retnla/ Fizz1
ctr
HpbE
Relative gene expression
0.3
0.2
0.1
0.0
p=0.06
0.25
0.20
0.15
0.10
0.05
0.00
p=0.06
0.04
0.03
0.02
0.01
0.00
p=0.06
5x10-5
4x10-5
3x10-5
2x10-5
1x10-5
0
1x10-4
8x10-5
6x10-5
4x10-5
2x10-5
0

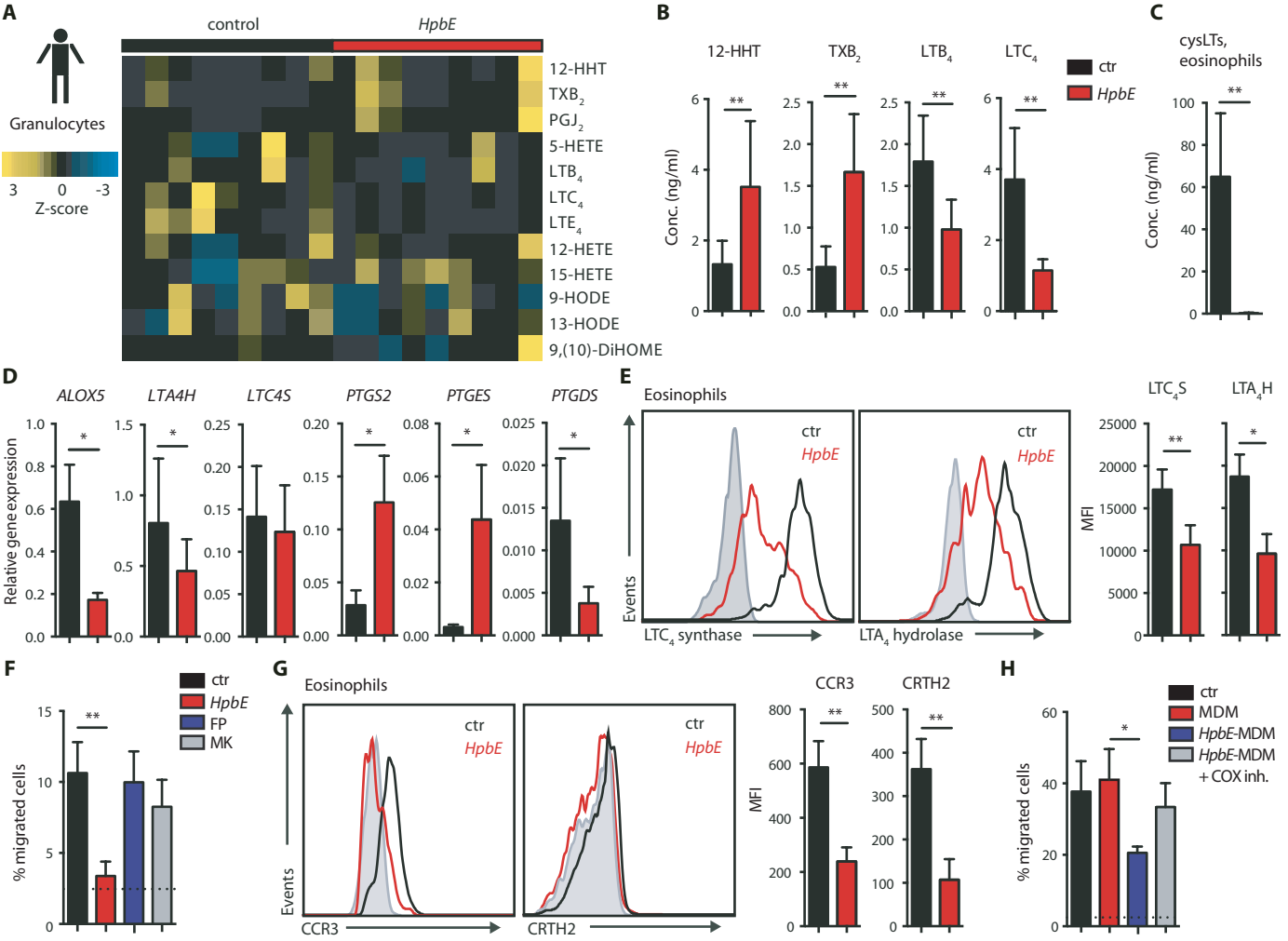
A
control
HpbE
Granulocytes
3
0
-3
Z-score
12-HHT
TXB2
PGJ2
5-HETE
LTB4
LTC4
LTE4
12-HETE
15-HETE
9-HODE
13-HODE
9,(10)-DiHOME
B
12-HHT
TXB2
LTB4
LTC4
ctr
HpbE
Conc. (ng/ml)
C
cysLTs, eosinophils
Conc. (ng/ml)
D
ALOX5
LTA4H
LTC4S
PTGS2
PTGES
PTGDS
Relative gene expression
E
Eosinophils
ctr
HpbE
Events
LTC4 synthase
LTA4 hydrolase
LTC4S
LTA4H
MFI
F
ctr
HpbE
FP
MK
% migrated cells
G
Eosinophils
ctr
HpbE
Events
CCR3
CRTH2
MFI
H
ctr
MDM
HpbE-MDM
HpbE-MDM + COX inh.
% migrated cells

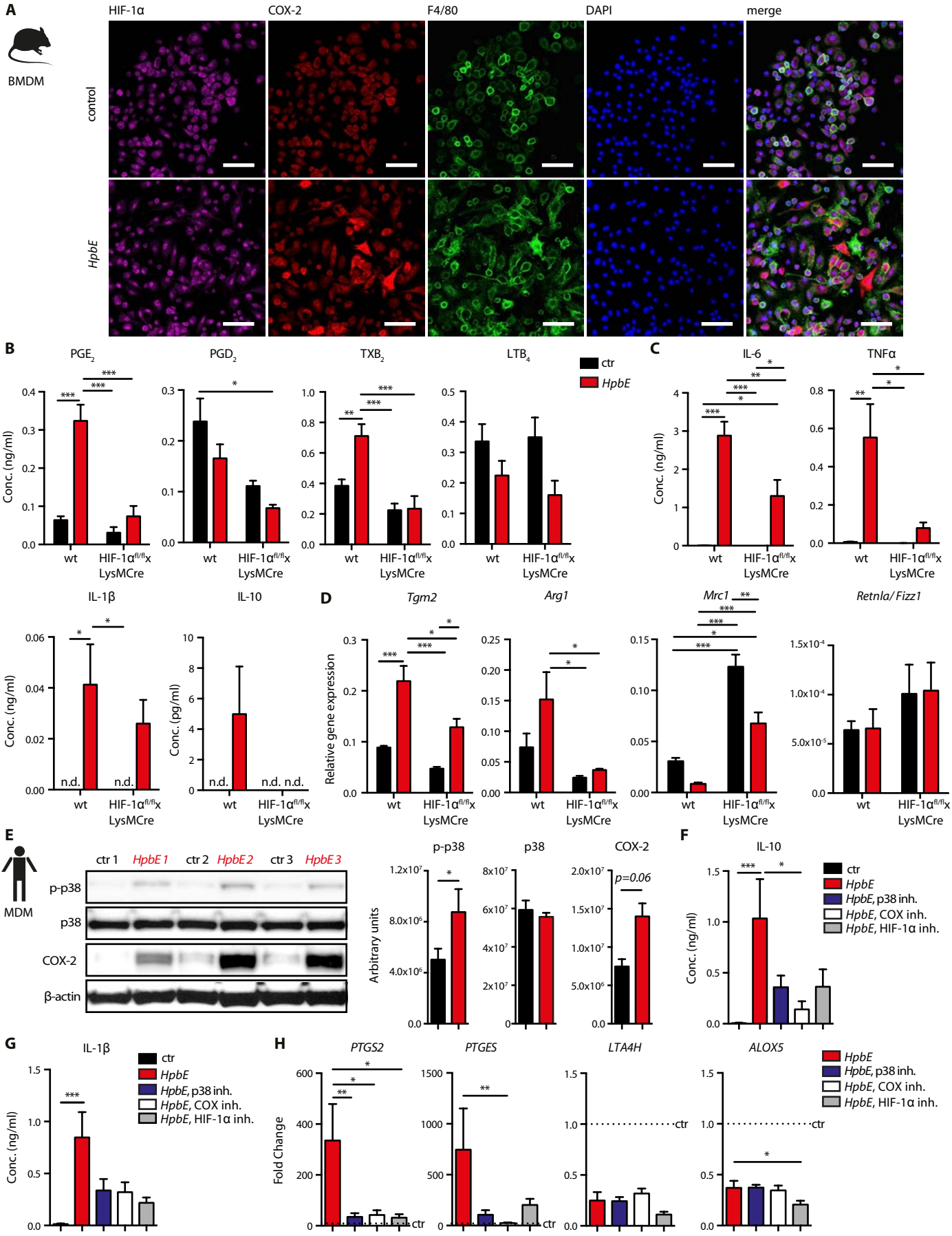
A
HIF-1α
COX-2
F4/80
DAPI
merge
BMDM
control
HpbE
B
PGE2
PGD2
TXB2
LTB4
ctr
HpbE
Conc. (ng/ml)
wt
HIF-1αfl/flx LysMCre
C
IL-6
TNFα
IL-1β
IL-10
Conc. (pg/ml)
n.d.
D
Tgm2
Arg1
Mrc1
Retnla/ Fizz1
Relative gene expression
E
MDM
ctr 1
HpbE 1
ctr 2
HpbE 2
ctr 3
HpbE 3
p-p38
p38
COX-2
β-actin
Arbitrary units
p=0.06
F
HpbE, p38 inh.
HpbE, COX inh.
HpbE, HIF-1α inh.
G
H
PTGS2
PTGES
LTA4H
ALOX5
Fold Change

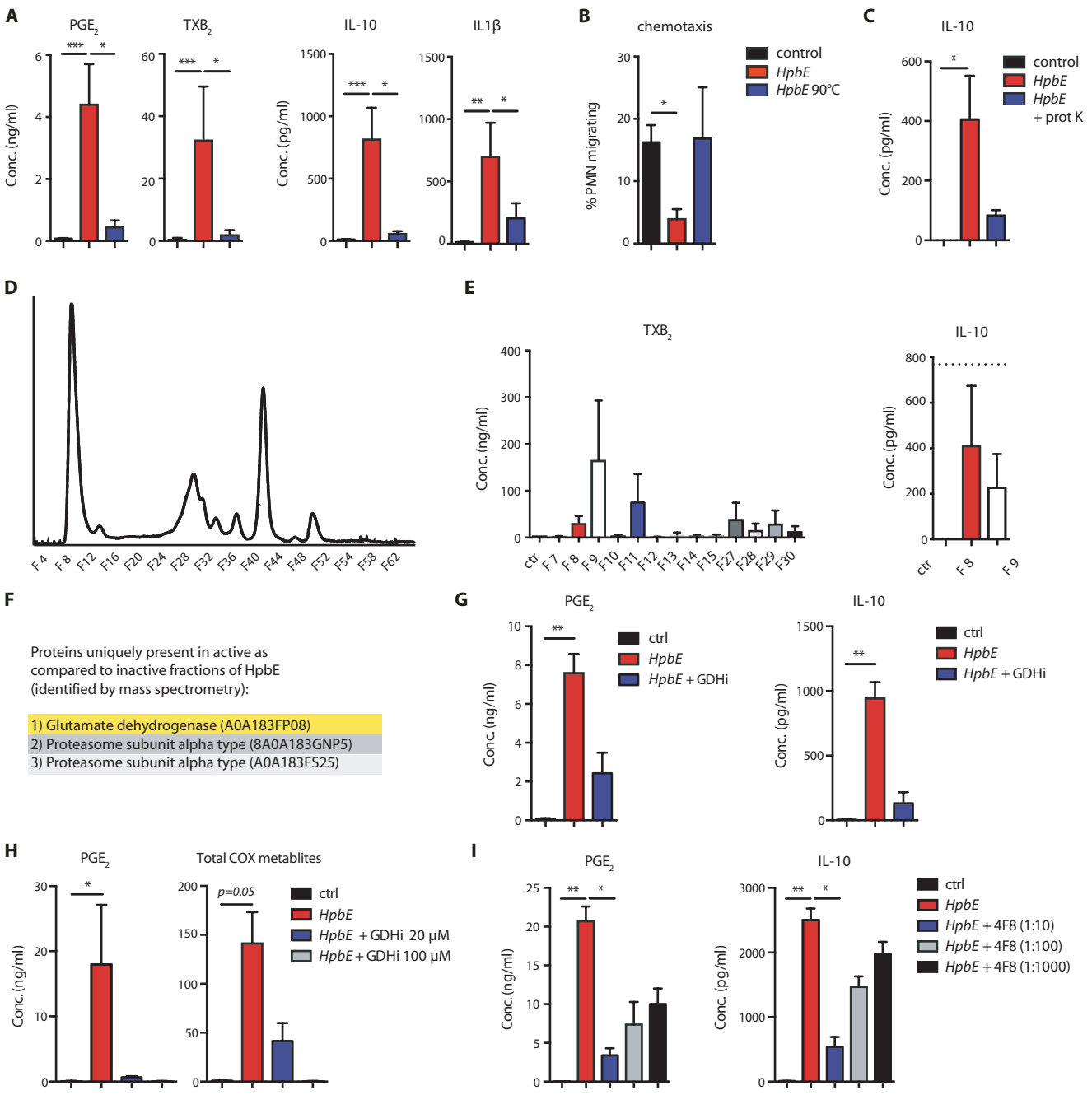
A
PGE2
TXB2
IL-10
IL1β
Conc. (ng/ml)
Conc. (pg/ml)
B
chemotaxis
% PMN migrating
control
HpbE
HpbE 90°C
C
IL-10
Conc. (pg/ml)
control
HpbE
HpbE + prot K
D
F 4 F 8 F12 F16 F20 F24 F28 F32 F36 F40 F44 F48 F52 F54 F58 F62
E
TXB2
IL-10
Conc. (ng/ml)
Conc. (pg/ml)
ctr F 7 F 8 F 9 F10 F11 F12 F13 F14 F15 F27 F28 F29 F30
ctr F 8 F 9
F
Proteins uniquely present in active as compared to inactive fractions of HpbE (identified by mass spectrometry):
1) Glutamate dehydrogenase (A0A183FP08)
2) Proteasome subunit alpha type (8A0A183GNP5)
3) Proteasome subunit alpha type (A0A183FS25)
G
PGE2
IL-10
Conc. (ng/ml)
Conc. (pg/ml)
ctrl
HpbE
HpbE + GDHi
H
PGE2
Total COX metablites
p=0.05
Conc. (ng/ml)
ctrl
HpbE
HpbE + GDHi 20 µM
HpbE + GDHi 100 µM
I
PGE2
IL-10
Conc. (ng/ml)
Conc. (pg/ml)
ctrl
HpbE
HpbE + 4F8 (1:10)
HpbE + 4F8 (1:100)
HpbE + 4F8 (1:1000)

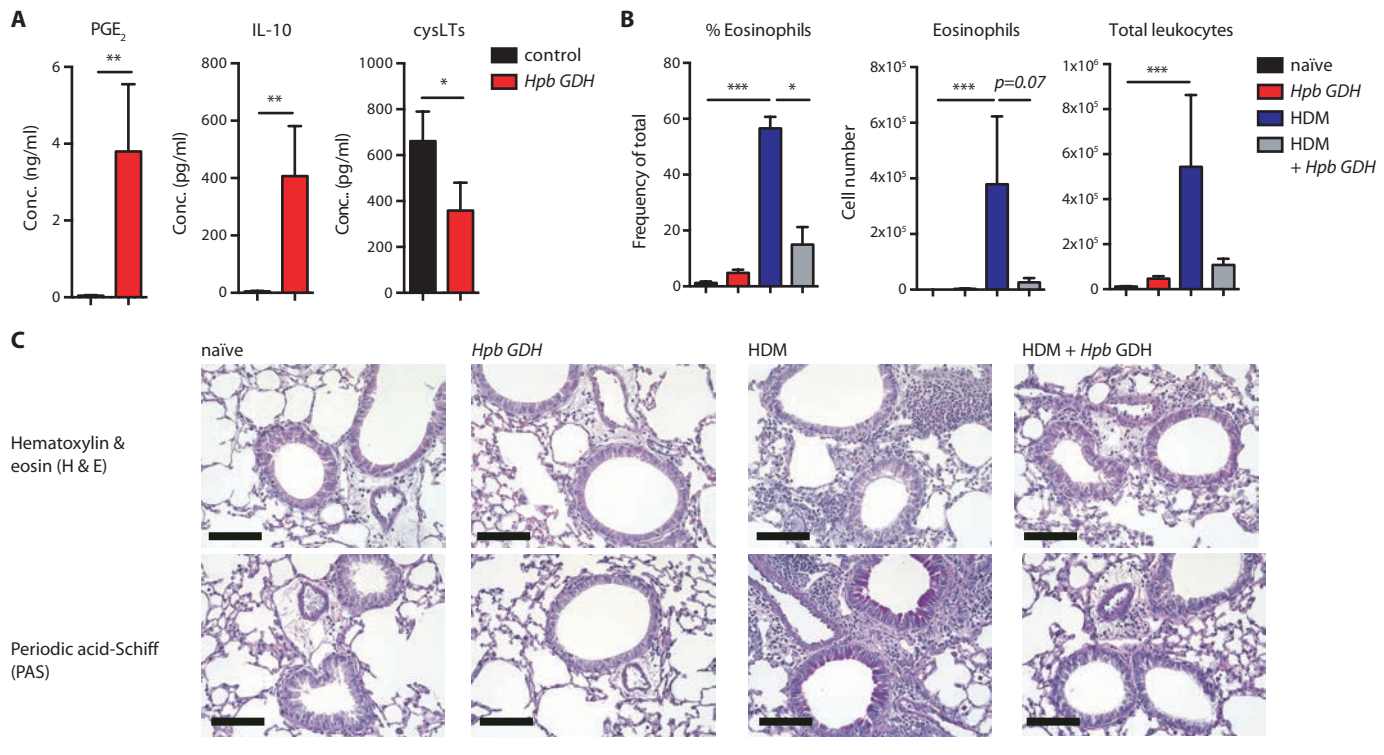
A
PGE2
IL-10
cysLTs
control
Hpb GDH
Conc. (ng/ml)
Conc. (pg/ml)
Conc. (pg/ml)
**
**
*
B
% Eosinophils
Eosinophils
Total leukocytes
Frequency of total
Cell number
***
*
***
p=0.07
***
naïve
Hpb GDH
HDM
HDM
+ Hpb GDH
C
naïve
Hpb GDH
HDM
HDM + Hpb GDH
Hematoxylin &
eosin (H & E)
Periodic acid-Schiff
(PAS)

Supplementary information

Title: An anti-inflammatory eicosanoid switch mediates the suppression of type-2 inflammation by helminth larval products

Authors: Marta de los Reyes Jiménez[1*], Antonie Lechner[1*], Francesca Alessandrini[1], Sina Bohnacker[1], Sonja Schindela[1], Aurélien Trompette[2], Pascal Haimerl[1], Dominique Thomas[3], Fiona Henkel[1], André Mourão[4], Arie Geerlof[4], Clarissa Prazeres da Costa[5], Adam M Chaker[6], Bernhard Brüne[7], Rolf Nüsing[7], Per-Johan Jakobsson[8], Wolfgang A Nockher[9], Matthias J Feige[10], Martin Haslbeck[11], Caspar Ohnmacht[1], Benjamin J Marsland[12], David Voehringer[13], Nicola L Harris[12], Carsten B Schmidt-Weber[1,14], Julia Esser-von Bieren[1#]

[*] These authors contributed equally

[#] To whom correspondence should be addressed: Julia.esser@helmholtz-muenchen.de

Supplementary materials and methods

Identification of *Hpb*-associated bacteria

Hpb extract was plated on Columbia and McConkey Agar plates (for aerobic bacteria) and KV (Kanamycin/Vancomycin) and Schaedler plates (anaerobic bacteria) (all plates from Biomerieux) and incubated at 5% CO_2 or in anaerobic chambers for 48 hrs at 36°C. No anaerobic growth was observed. Aerobic bacteria (*Bacillus cereus, Enterococcus faecalis, Paenibacillus odorifer, Stenotrophomonas maltophilia)* were counted and identified with Maldi-TOF-MS (Microflex, Bruker). A suspension with a mix of bacteria at identical concentrations as in the original *Hpb* extract was prepared in broth prior to use in cell culture.

Schistosoma mansoni infection and preparation of larval extract

For experimental infection of mice with *Schistosoma mansoni (S.m.)*, cercaria from a Brazilian strain of *S.m*. were isolated from *Biomphalaria glabrata* snails (Brazilian origin), and mice were infected intraperitoneally with 100–140 cercariae, as previously described *(41)*. *Schistosoma mansoni* (*S.m.)* extract was prepared from newly transformed schistosomula (NTS) as previously published *(41)*. In brief, cercariae from a Brazilian strain of *S.m*. were isolated from *Biomphalaria glabrata* snails using the light induction method as previously described *(41)*. After thorough washing, cercariae were re-suspended in ice-cold HBSS medium, pipetted vigorously and vortexed three minutes at the highest speed to trigger tail loss, which was confirmed by microscopy. NTS were then cultured in hybridoma medium (Biochem) at 37°C, 5% CO_2 in ambient air for 7 days. At this timepoint all NTS had transformed into lung stage larvae. These were harvested and homogenized in culture medium using Precellys tough micro-organism lysing kits (Bertin Pharma) at 6000 rpm for 30 sec in two cycles. Debris were removed by centrifugation at 13.000 rpm for 20 min.

Generation and stimulation of BMDM

Bone marrow derived macrophages (BMDM) from bone marrow of wildtype C57BL/6 or HIF-1$\alpha^{floxed/floxed}$xLysMCre mice were isolated and cultured for 6 days in the presence of murine recombinant GM-CSF (10 ng/ml) (Miltenyi Biotech) and human recombinant TGF-β1 (2 ng/ml) (Peprotech) as previously described *(54)*. On day 6, cells were harvested and used for further experiments. When mentioned, BMDM were stimulated with 10 µg/ml *HpbE*. After overnight stimulation, BMDM

were stimulated with 5 μM Ca^{2+}-ionophore A23187 (Sigma Aldrich) for 10 min and supernatants were stored at -80ºC in 50% MeOH for LC-MS/MS analysis or undiluted for cytokine analysis. Cell pellets were lysed in RLT buffer with 1% β-mercaptoethanol (Merck Millipore) and stored at -80ºC until RNA extraction.

Transfer of Bone Marrow-derived Macrophages during HDM-induced allergic airway inflammation

Eight weeks old female C57BL/6 mice were sensitized i.n. with HDM extract on day 0. For the transfer experiment, BMDM from bone marrow of wildtype C57BL/6, *ptges*$^{-/-}$ or *ptgs2*$^{-/-}$ mice *(56)* were isolated and differentiated for 6 days in the presence of murine recombinant GM-CSF and human recombinant TGF-β1. BMDM (wt, *ptges*$^{-/-}$ or *ptgs2*$^{-/-}$) were pooled from 3 mice and incubated for 24 h in the presence or absence of 10 μg/ml *HpbE*. 45 min before intranasal transfer, BMDM were harvested by scraping, washed and resuspended in PBS. On days 10-13, mice received PBS or $3x10^5$ BMDM (wt, *ptges*$^{-/-}$ or *ptgs2*$^{-/-}$) +/- *HpbE* in 20 μl PBS i.n. before HDM or mock challenge. Mice were sacrificed 18 h after the last challenge. BALF was collected using 0.5 ml PBS and stored as described in the Materials and Methods section of the main text.

Generation and stimulation of Monocyte-derived Macrophages

Monocyte-derived macrophages (MDM) were generated from $CD14^+$ PBMCs, as described previously *(6)*. MDM were cultured in the presence of 10 ng/ml human

GM-CSF (Miltenyi Biotech) and 2 ng/ml human TGF-β1 (Peprotech). On day 6, cells were harvested by scraping and used for further experiments. When indicated, cells were stimulated overnight with 10 µg/ml parasite products (*HpbE*, *SmE*, HES, L4 extract, L5 extract) or 5 µg/ml protein (*Hpb* GDH). When mentioned, *HpbE* was pre-treated with 200 µg/ml proteinase K over night at 37 °C prior to stimulation of MDM. Eicosanoid production was elicited by stimulating cells with 5 µM ionophore A23187 for 10 min at 37°C. For inhibitor studies, the following pharmacological inhibitors where added as indicated before *Hpb*E stimulation: 5 µM BAY 11-7085 (Enzo Life Sciences), 10 µM CAY10404, 10 µM H-89, 100 µM Indomethacin, 250 nM SF1670, 1 µM VX-702, 100 nM Wortmannin (Cayman Chemical), 3 µM Acriflavine, 20 or 100 µM Bithionol (Sigma-Aldrich). For experiments with neutralizing antibodies, MDM were incubated with 10 µg/ml anti-dectin-1 antibody, 10 µg/ml anti-dectin-2 antibody, 10 µg/ml anti-TLR2 antibody (all Invivogen), 5 µg/ml anti-IL-1β antibody (Abcam), or anti-*Hpb* GDH (clone 4F8) (1:100/ 1:1000/ 1:10000) or isotype control (1:100) before *HpbE* stimulation. When indicated, MDM were stimulated with 60 ng/ml LPS (Invivogen). When indicated, MDM were incubated with 1 µM Fluticasone Propionate or 1 µM Dexamethasone (Sigma Aldrich) one hour before *HpbE* treatment. Eicosanoid production was elicited by stimulating cells with 5 µM Ca^2+-ionophore A23187 (Sigma Aldrich) for 10 min and supernatants were stored at -80ºC in 50% MeOH for LC-MS/MS analysis or undiluted for cytokine analysis. Cell pellets were lysed in RLT buffer with 1% β-mercaptoethanol (Merck Millipore) and stored at -80ºC for RNA extraction. In some experiments, cell pellets were lysed with

RIPA buffer and stored at -80ºC for Western blot or MDM were fixed and stained for immunofluorescence.

Isolation and stimulation of human PBMCs

PBMCs were isolated by centrifugation on Polymorphprep-density gradients (Axis-Shield). When indicated, $CD14^+$ PBMCs were isolated by magnetic bead separation using $CD14^+$ MACS beads (Miltenyi Biotech), and the negative fraction was used as $CD14^-$ PMBCs. PBMC, $CD14^+$ PBMCs or $CD14^-$ PBMCs were resuspended in medium in the presence of 10 ng/ml human GM-CSF (Miltenyi Biotech), and stimulated overnight with 10 µg/ml *Hpb*E. After overnight treatment, cells were stimulated with 5 µM $Ca2^+$-ionophore A23187 (Sigma Aldrich) for 10 min. Cell supernatants were stored at -80ºC in 50% MeOH for LC-MS/MS or undiluted for cytokine analysis. Cell pellets were lysed in RLT buffer with 1% β-mercaptoethanol (Merck Millipore) and stored at -80ºC for RNA extraction.

Isolation and stimulation of human PMN and eosinophils

PMN were isolated by centrifugation on Polymorphprep-density gradients (Axis-Shield). Eosinophils were isolated using an Eosinophil Isolation kit (Miltenyi Biotech). Eosinophils or PMN were resuspended in medium in the presence of 100 ng/ml human GM-CSF (Miltenyi Biotech), and stimulated overnight with 10 µg/ml *Hpb*E. When mentioned, PMN were treated with 1 µM fluticasone propionate or dexamethasone (Sigma Aldrich). After overnight treatment, PMN or eosinophils were

stimulated with 5μM Ca^{2+}-ionophore A23187 (Sigma Aldrich) for 10 min. Cell supernatants were stored at -80ºC in +/-50% MeOH for LC-MS/MS or cytokine analysis. Cell pellets were lysated in RLT buffer with 1% β-mercaptoethanol (Merck Millipore) and stored at -80ºC until RNA extraction. In some experiments, cells were stained for flow cytometry analysis.

Chemotaxis assays

PMN were resuspended to a concentration of $1x10^6$ cells/ml in the presence of 100 ng/ml human GM-CSF (Miltenyi Biotech) and stimulated overnight with 10 μg/ml *HpbE* or heat-inactivated *HpbE*. When mentioned, PMN were pre-treated with 1 μM fluticasone propionate (Sigma-Aldrich), 10 μM montelukast (Cayman Chemical) or conditioned media from MDM stimulated overnight with 10 μg/ml *Hpb* extract +/- 100 μM indomethacin for 1 hour. PMN migration in response to nasal polyp secretions or a chemokine cocktail of 2 ng/ml RANTES, 20 ng/ml IL-8 (Miltenyi Biotech) and 2 ng/ml LTB_4 (Cayman Chemical) was tested. Chemoattractants were placed in the lower wells of a chemotaxis plate (3 μm pore size; Corning). After mounting the transwell unit, $2x10^5$ PMN were added to the top of each transwell and migration was allowed for 3 hours at 37°C, 5% CO_2. The number of cells migrating to the lower well was counted microscopically. In some experiments, manual counting was validated by flow cytometry.

Quantitative Real-Time PCR

Total RNA was isolated by using the Quick-RNA MicroPrep Kit (Zymo Research) according to the manufacturer's protocol. Isolated total RNA was subjected to reverse transcription by using a high-capacity cDNA kit (Thermo Fisher Scientific). Real-time PCR was performed using a ViiA 7 Real-Time PCR System (Applied Biosystems, Thermo Fisher Scientific) and the FastStart Universal SYBR Green Master Mix (Roche). Transcript levels were normalized to *GAPDH*. Primer sequences for the genes of interest are available in Supplementary Table 3.

Histology and immunofluorescence stainings

Lung- or small intestinal tissues were fixed in 10% formalin, paraffin embedded and sectioned using a microtome (Leica Microsystems). For hematoxylin and eosin (H&E)- or Periodic acid-Schiff (PAS) staining, lung tissues were fixed and stained as described previously *(56)*.

For immunofluorescence staining, cells were fixed for 15 minutes with 4% paraformaldehyde, followed by permeabilization with acetone (10 minutes at -20°C). After blocking with 5% BSA and 10% donkey serum, cells were incubated with primary antibodies against goat anti-human cyclooxygenase-2 (Cayman Chemical), rabbit anti-human HIF-1α and rat anti-mouse F4/80 (Thermo Fisher). Fluorescence-conjugated secondary antibodies were used for detection (see Table S4). Images were recorded on an EVOS system (Thermo Fisher Scientific) or a Leica SP5 confocal microscope (Leica Microsystems).

Western Blotting

Immunoblotting was performed as described previously *(6)*. In brief, cells were lysed in RIPA buffer (Thermo Fisher Scientific) supplemented with 4% EDTA-free complete protease inhibitor cocktail and 10% phosphatase inhibitor cocktail (both Roche Applied Science). The protein concentration was determined by the BCA method (Thermo Fisher Scientific) and lysates were diluted to equal concentrations. NuPAGE LDS Sample buffer and NuPAGE Sample Reducing Agent (Thermo Fisher Scientific) was added to total lysates and heated at 70 °C for 10 minutes. Samples were loaded on Bolt 4-12% Bis-Tris Plus gels (Thermo Fisher Scientific) and separated by electrophoresis. Gels were transferred to a PVDF membrane (Merck Chemical) and blocked in 5% nonfat dry milk in 1x TBS containing 0.02% Tween for 1 hour to prevent unspecific binding. Membranes were incubated overnight with primary antibodies against phospho-p38 and p38 (both Cell Signaling, dilution 1:1000), COX-2 (Cayman Chemical, dilution: 1:1000) or β-actin (Sigma-Aldrich, dilution 1:10000), washed and incubated with the corresponding secondary horseradish peroxidase-conjugated antibody. Detection was performed using enhanced chemiluminescence (SuperSignal West Femto Maximum Sensitivity Substrate, Pierce, Thermo Fisher Scientific, or Amersham ECL Prime, GE Healthcare Life Technologies) and recorded with the ECL Chemocam Imager (Intas Science Imaging Instruments). LabImage 1D software (Kapelan Bio-Imaging) was used to quantify the protein levels by means of normalization and correction for the amount of β-actin in the samples.

Enzyme immunoassays (EIA)

The concentration of LTB_4, CysLTs, PGE_2 and TXB_2 in culture supernatants was determined by using commercially available enzyme immunoassay (EIA) kits (Cayman Chemical), according to the manufacturer's instruction.

ELISA

Cell culture supernatants were analyzed for IL-10 or IL-1β secretion using the human IL-10 or IL1-β ELISA Set (BD Biosciences), according to the manufacturer's instructions.

Bioplex Assay

Mouse cell culture supernatants were analyzed by Multiplex cytokine assays (Bioplex Pro Reagent Kit V, Biorad) for the detection of murine IL-1β, IL-6, IL-10, Eotaxin (CCL11), IL-13, RANTES (CCL5) and TNFα. Human cell culture supernatants were analyzed by Magnetic Luminex Assay (R&D Systems) for the detection of human Eotaxin (CCL11), GROα (CXCL1), GROβ (CXCL2), IL-1β, IL-18, IL-6, TARC (CCL17), IP-10 (CXCL10), IL-8 (CXCL8), IL-10, IL-27, TNFα, RANTES (CCL5), ITAC-1 (CXCL11), MIG (CXCL9), IL-12 p70 and IL-33. Both commercially available kits were performed according to the manufacturer's instructions on a Bio-Plex 200 System (Bio-Rad).

LC-MS/MS analysis of PUFA metabolites

Cell culture or BALF supernatants were adjusted to 10% methanol containing deuterated internal standard followed by an extraction using solid reverse phase extraction columns (Bond Elut Plexa 30 mg, Agilent). Samples were eluted into 1.0 ml of methanol, lyophilized and resuspended in 100 µl of water/acetonitrile/formic acid (70:30:0.02, v/v/v; solvent A) and analyzed by LC-MS/MS on an Agilent 1290 liquid chromatography separation system. Separation was performed on a Synergi Hydro reverse-phase C18 column (2.1×250 mm; Phenomenex) using a gradient as follows: flow rate =0.3 µl/min, 1 min (acetonitrile/isopropyl alcohol, 50:50, v/v; solvent B), 3 min (25% solvent B), 11 min (45% solvent B), 13 min (60% solvent B), 18 min (75% solvent B), 18.5 min (90% solvent B), 20 min (90% solvent B), 21 min (0% solvent). The separation system was coupled to an electrospray interface of a QTrap 5500 mass spectrometer (AB Sciex). For inhibitor experiments, a smaller LC-MS/MS panel was used. Briefly, analytes were separated under gradient conditions within 16 min: 1 min (90% solvent A), 2 min (60% solvent A), 3 min (50% solvent A), 3 min (10% solvent A). Within 1 min, the initial conditions were restored and the column was re-equilibrated for 6 min. Mass spectrometric parameters were as follows: Ionspray voltage -4500 V, source temperature 500 °C, curtain gas 40 psi, nebulizer gas 40 psi and Turbo heater gas 60 psi. Both quadrupoles were running at unit resolution. Compounds were detected in scheduled multiple reaction monitoring mode. For quantification a 12-point calibration curve for each analyte was used. Data analysis was performed using Analyst (v1.6.1) and MultiQuant (v2.1.1) (AB Sciex).

Fractionation and mass spectrometry analysis of *Hpb* larval extract

Soluble protein fractions were separated by gel filtration chromatography (SEC) on a Superdex 75 10/300 GL column with the ÄKTA pure system (GE Health Care Life Science). 300 µl of *Hpb* extract was loaded onto the column and eluted isocratically with PBS (pH=8), flow rate 0.8 ml/min. Fractions of 0.5 ml were collected starting when protein presence was detected at λ = 280 nm. Fractions from the SEC were prepared for liquid chromatography-mass spectrometry analysis, as described previously *(58, 59)*. Proteins in the samples were reduced, alkylated and digested overnight with trypsin. Peptides were extracted in five steps by sequentially adding 200 µl of buffer A (0.1% formic acid in water), acetonitrile (ACN), buffer A, ACN, ACN respectively. After each step samples were treated for 15 min by sonication. After steps 2, 4 and 5, the supernatant was removed from the gel slices and collected for further processing. The collected supernatants were pooled, evaporated to dryness in a speed vac (DNA 120, ThermoFisher Scientific) and stored at -80°C. For the MS measurements the samples were dissolved by adding 24 µl of buffer A and sonicated for 15 min. The samples were then filtered through a 0.22-µm centrifuge filter (Merck Millipore). Peptides were loaded onto an Acclaim PepMap RSLC C18 trap column (Trap Column, NanoViper, 75 µm x 20 mm, C18, 3 µm, 100 Å, ThermoFisher Scientific) with a flow rate of 5 µL/min and separated on a PepMap RSLC C18 column (75 µm x 500 mm, C18, 2 µm, 100 Å, ThermoFisher Scientific) at a flow rate of 0.3 µL/min. A double linear gradient from 5 % (vol/vol) to 28 % (vol/vol) buffer B (acetonitrile with 0.1 % formic acid) in 30 min and from 28% (vol/vol) to 35 % (vol/vol) buffer B in 5 min eluted the peptides to an Orbitrap

QExactive plus mass spectrometer (ThermoFisher Scientific). Full scans and five dependent collision-induced dissociation MS2 scans were recorded in each cycle.

The mass spectrometry data derived from the SEC fractions were searched against the Swiss-Prot *Heligmosomoides polygyrus bakeri* Database downloaded from UniProt (24.01.2017 edition) using the Sequest HT Algorithm implemented into the "Proteome Discoverer 1.4" software (ThermoFisher Scientific). The search was limited to tryptic peptides containing a maximum of two missed cleavage sites and a peptide tolerance of 10 ppm for precursors and 0.04 Da for fragment masses. Proteins were identified with two distinct peptides with a target false discovery rate for peptides below 1% according to the decoy search. Proteins detected in the negative control samples were subtracted from the respective hit-lists. For further evaluation two independent datasets resulting from SEC separations of biological replicates were combined. Only hits that were observed in both datasets were taken into account.

Cloning, expression and purification of *Hpb* GDH

Preparation of the expression construct

The *Hpb GDH* gene was amplified by PCR using Pfu polymerase and a pET-21a/Hpb GDH construct (GeneArt, Thermo Fisher) as a template.

For the amplification the following primers were used: GDHfw, GAATCTTTATTTTCAGGGCGCCATGCTGAGCACCCTGGCAC and GDHrev, GAGCTCGAATTCGGATCCGGTACCTTATTAGGTAAAGGTAAAACCTGC.

The obtained PCR product was cloned into a linearized pETM-11 vector

(https://www.helmholtz-muenchen.de/pepf/home/index.html) using the SLiCe method *(60)*. The expression construct was verified by sequencing.

Protein expression and purification

The pETM-11/Hpb GDH construct was transformed into *E. coli* strain BL21 (DE3) cc4, overexpressing the (co-)chaperones GroEL, GroES, DnaK, DnaJ, GrpE and ClpB *(61)* and cultured at 20°C in a 2-L flask containing 500 ml ZYM 5052 auto-induction medium *(62)* and 30 µg/ml kanamycin, 50 µg/ml spectinomycin and 10 µg/ml chloramphenicol. Cells were harvested by centrifugation after reaching saturation, resuspended in 40 ml lysis buffer (50 mM Tris-HCl, 300 mM NaCl, 20 mM imidazole, 10 mM $MgCl_2$, 10 µg/ml DNaseI, 1 mM AEBSF.HCl, 0,2% (v/v) NP-40, 1 mg/ml lysosyme, 0.01% (v/v) 1-thioglycerol, pH 8.0), and lysed by sonication. The lysate was clarified by centrifugation (40,000 x g) and filtration (0.2 µM). The supernatant was applied to a 5-ml HiTrap Chelating HP column (GE Healthcare), equilibrated in buffer A (50mM Tris-HCl, 300mM NaCl, 20mM imidazole, 0.01% (v/v) 1-thioglycerol, pH 8.0) using an Äkta Purifier (GE Healthcare). The column was washed with buffer A and buffer A containing 50mM imidazole until a stable baseline was reached (monitored at 280nm). Bound proteins were eluted with a linear gradient of from 50 to 300 mM imidazole in buffer A. Fractions containing GDH were pooled and dialyzed overnight at 4°C against 1 L buffer B (50mM Tris-HCl, 300mM NaCl, 0.01% (v/v) 1-thioglycerol, pH 8.0) in the presence of His-tagged TEV protease in a 1:25 molar ratio (TEV:protein). The cleaved off GDH was further purified by affinity chromatography as described above

and the flow-through and protein containing wash fractions were pooled and concentrated to less than 2 ml. This was subsequently subjected to two runs of size exclusion chromatography using a Superdex 200 10/300 GL column (GE Healthcare), equilibrated in buffer B. The main elution peak containing GDH was collected and concentrated to approx. 2 mg/ml and stored at 4°C. Protein concentrations were determined by measuring the absorbance at 280 nm using the specific absorbance for *Hpb* GDH of 1.057 ml/mg.cm.

Generation of monoclonal antibodies against *Hpb* GDH

Rats were immunized against two different peptides specifically found in GDH of *Hpb*, but not mammalian GDH (peptides A and B are specified in Figure 4). The subsequent steps (fusion, hybridoma screening and subcloning) were carried out according to standard procedures of the monoclonal antibody core facility at the Helmholtz Center Munich (https://www.helmholtz-muenchen.de/mab/how-we-work/index.html). Westernblot analysis was performed according to previously published protocols *(6)*.

Flow cytometry

After overnight stimulation with 10 µg/ml *HpbE*, human eosinophils were stained with APC-labeled antibodies against LTC_4S or LTA_4H (both Santa Cruz Biotechnologies) (prepared by using an antibody conjugation kit, Innova Biosciences, according to the manufacturer's instructions) as well as with anti-human CCR3 (PE) and anti-CRTH2 (PE-CF594) antibodies (both BD Biosciences). Isotype-matched

antibodies were used as controls. All samples were acquired in a BD LSRFortessa^{TM} (BD Biosciences, California, United States) and analyzed by using FlowJo v10 software (FlowJo LLC, Freestar Inc.)

Glutamate Dehydrogenase activity assay

GDH activity was measured in human macrophages or helminth homogenates using the Glutamate Dehydrogenase (GDH) Activity Assay kit (Sigma), according to the manufacturer´s instructions.

LDH cytotoxicity assay

The cellular toxicity of the inhibitor bithionol in human macrophages was quantified using the LDH cytotoxicity assay kit (Thermo Scientific), according to the manufacturer´s instructions.

Supplementary figures

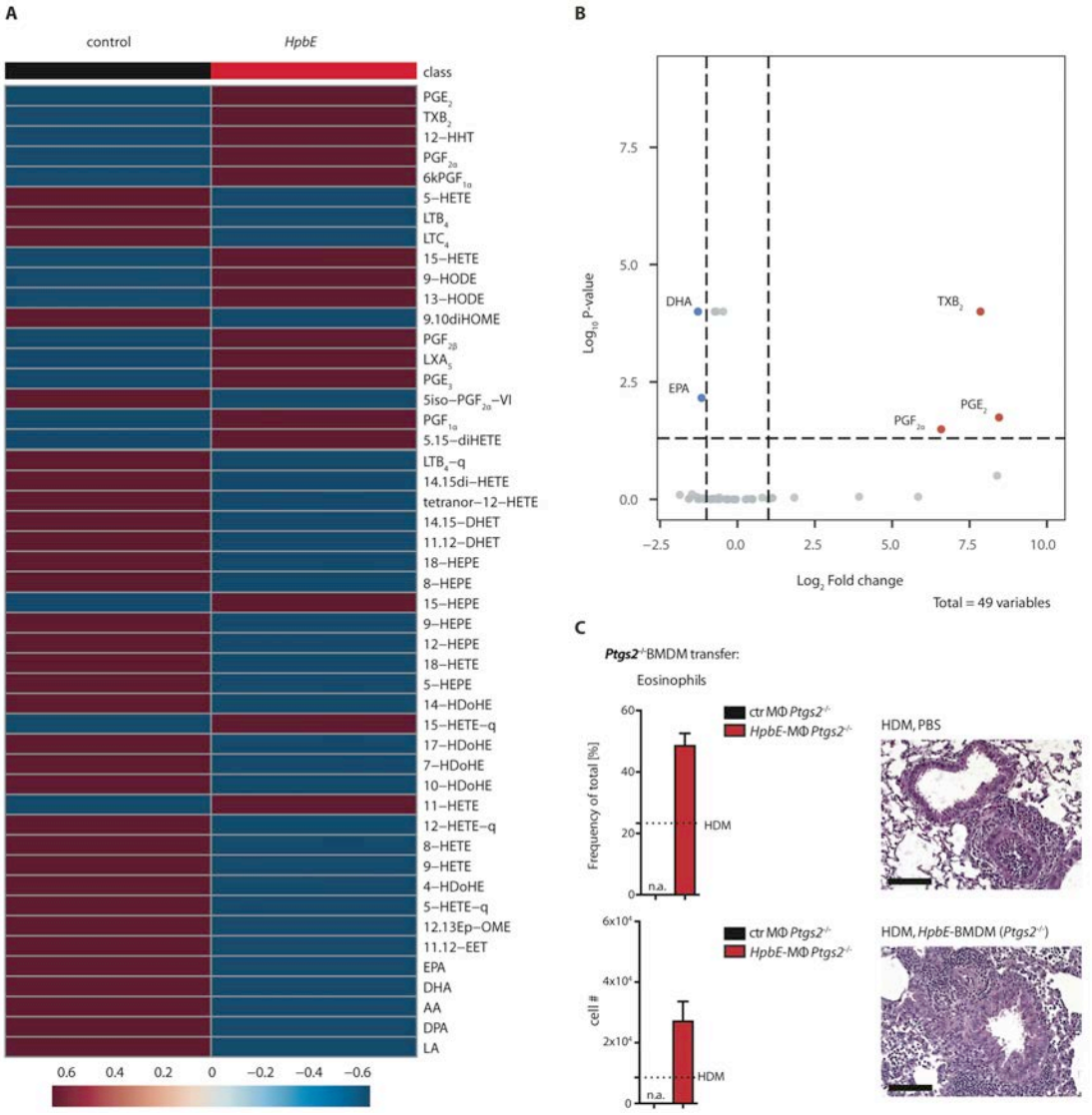

Fig. S1. Heat map and volcano plot of PUFA metabolites produced by human MDM in response to treatment with *HpbE* and impact of *HpbE*-treated *Ptgs2*$^{-/-}$ BMDM on eosinophilic airway inflammation

(**A**) Data are shown as average z-scores for MDM from 10 healthy human blood donors ± *HpbE* (24h) + A23187 (10 min). (**B**) Volcano plot of PUFAs and PUFA metabolites, significant changes (z-score), determined by ANOVA Fisher's LSD are

shown in blue (down) or red (up); thresholds were set to $p \leq 0.01$ and $\log_2$ Fold Change $\geq +1 / \leq -1$. (**C**) Left panels: frequencies and total numbers of eosinophils in BALF of mice sensitized to HDM + i.n. transfer of *HpbE*-conditioned *Ptgs2*$^{-/-}$ BMDM (MΦ) (n=4), 18h after the last challenge and transfer. Dashed lines indicate eosinophil levels in HDM-sensitized mice (mean of n=5); n.a. = not available. Right panels: representative H&E stained lung tissue from mice sensitized to HDM ± intranasal transfer of *HpbE*-conditioned BMDM (*Ptgs2*$^{-/-}$). Scale bar: 100 µm.

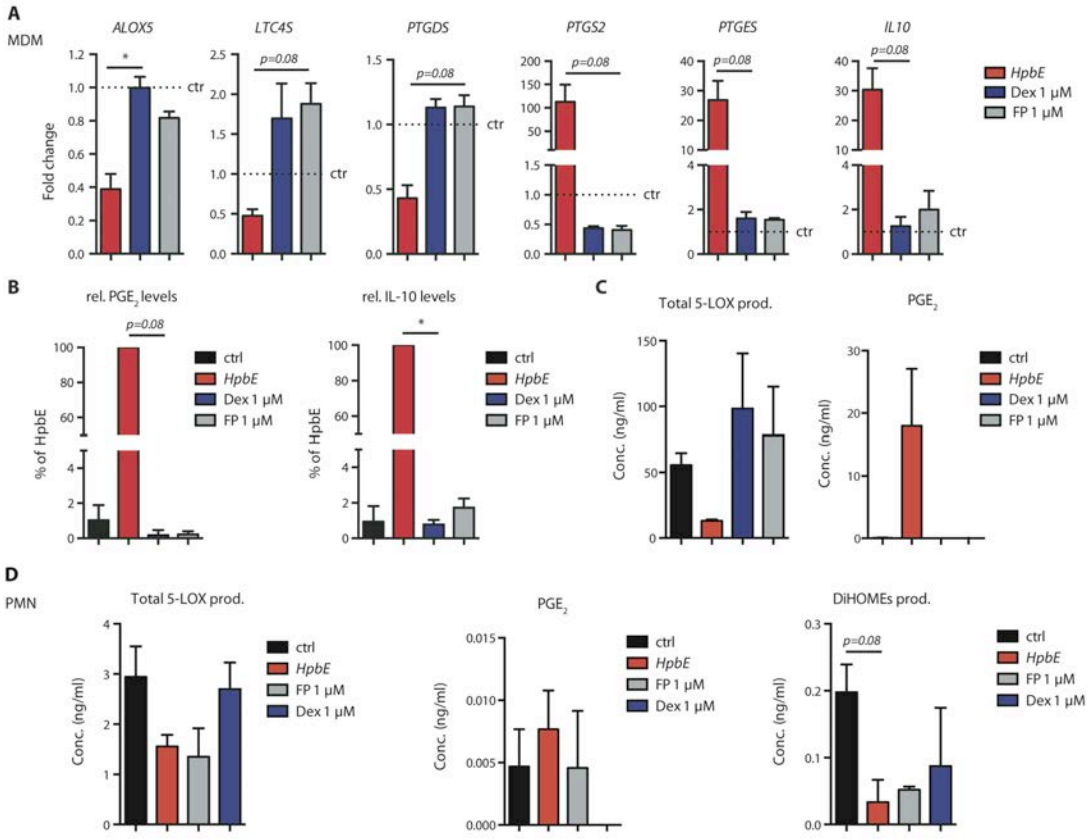

Fig. S2. *HpbE* has stronger eicosanoid-modulatory effects as compared to glucocorticosteroids.

(**A**) Fold change of eicosanoid pathway proteins or IL-10 (qPCR) in human MDM ± treatment with *HpbE*, Dexamethasone (Dex) or Fluticasone propionate (FP). (**B**)

Levels of PGE_2 (EIA) or IL-10 (ELISA) (normalized to levels for *HpbE*) in human MDM ± treatment with *HpbE*, Dexamethasone (Dex) or Fluticasone propionate (FP) (24h) + A23187 (10 min); (**C**) Levels of total 5-LOX products or PGE_2 (LC-MS/MS) produced by human MDM ± treatment with *HpbE*, Dexamethasone (Dex) or Fluticasone propionate (FP); (**D**) Levels of total 5-LOX products, PGE_2 or DiHOMEs (LC-MS/MS) produced by human PMN ± treatment with *HpbE*, Dexamethasone (Dex) or Fluticasone propionate (FP). Data are pooled from at least 2 independent experiments and presented as mean ± SEM for MDM from n=3-6 healthy human blood donors. Statistical significance was determined by Friedman test. *p<0.05.

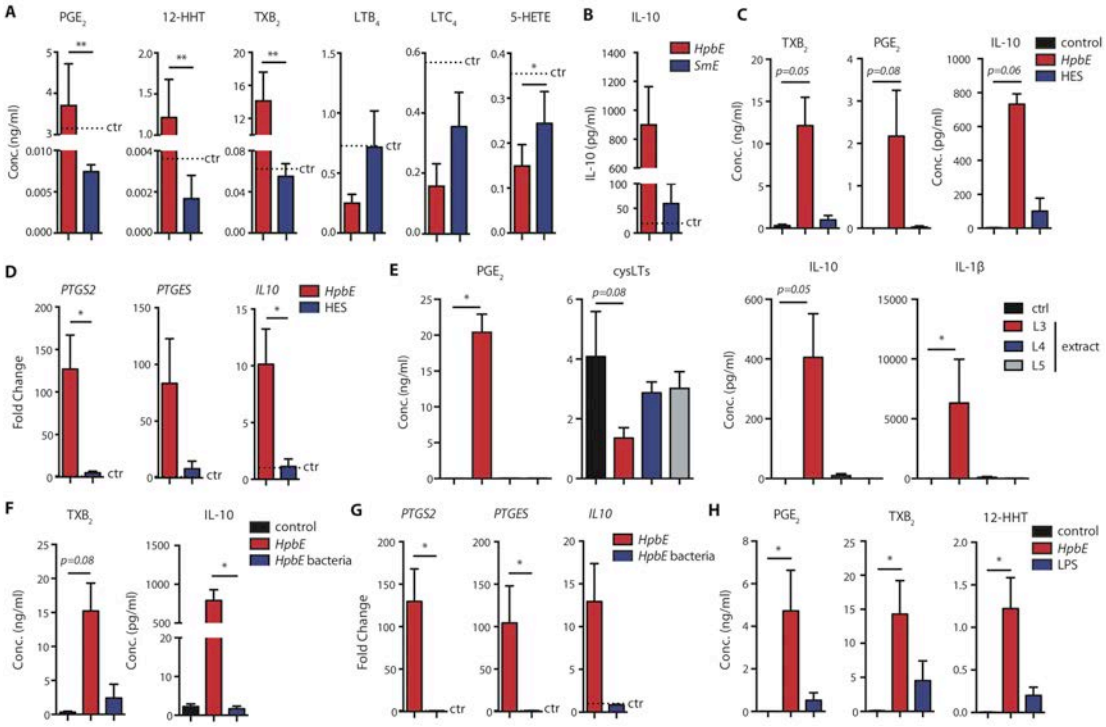

Fig. S3. *HpbE* has a unique potential to induce type-2-suppressive mediators compared to other helminth products or helminth-associated bacteria.

(**A**) Eicosanoid levels (LC-MS/MS) produced by human MDM after treatment with larval extracts from *Hpb* or *S. mansoni* (*SmE*) (24h) + A23187 (10 min). Dashed lines indicate control levels. (**B**) Levels of IL-10 (ELISA) produced by MDM ± treatment with *HpbE* or *SmE*. Dashed line indicates control level. (**C**) Levels of prostanoids (LC-MS/MS) or IL-10 (ELISA) in human MDM treated with *Hpb* larval extract (*Hpb*E) or *Hpb* excretory secretory products "HES" (10 μg/ml). (**D**) Relative gene expression of COX pathway enzymes or *IL10* (qPCR) in MDM treated with *HpbE* or HES. (**E**) Levels of PGE_2 or cysLTs (EIA) or IL-10 or IL-1β (Bioplex) produced by MDM ± treatment with L3, L4 or L5 extract of *Hpb*; (**F**) Levels of TXB_2 (EIA) or IL-10 (ELISA) produced by MDM after treatment with *HpbE* or a homogenate of major bacterial strains present in *HpbE*. (**G**) Relative gene expression of COX pathway enzymes or *IL10* (qPCR) in human MDM treated with *HpbE* or a homogenate of major bacterial strains present in *HpbE*. (**H**) Levels of prostanoids (LC-MS/MS) produced by MDM treated with *HpbE* or LPS (60 ng/ml). Results are expressed as mean ± SEM, n=3-6 per group. Statistical significance was determined by Wilcoxon test (two groups) or Friedman test (more than 2 groups). *$p < 0.05$, **$p < 0.01$.

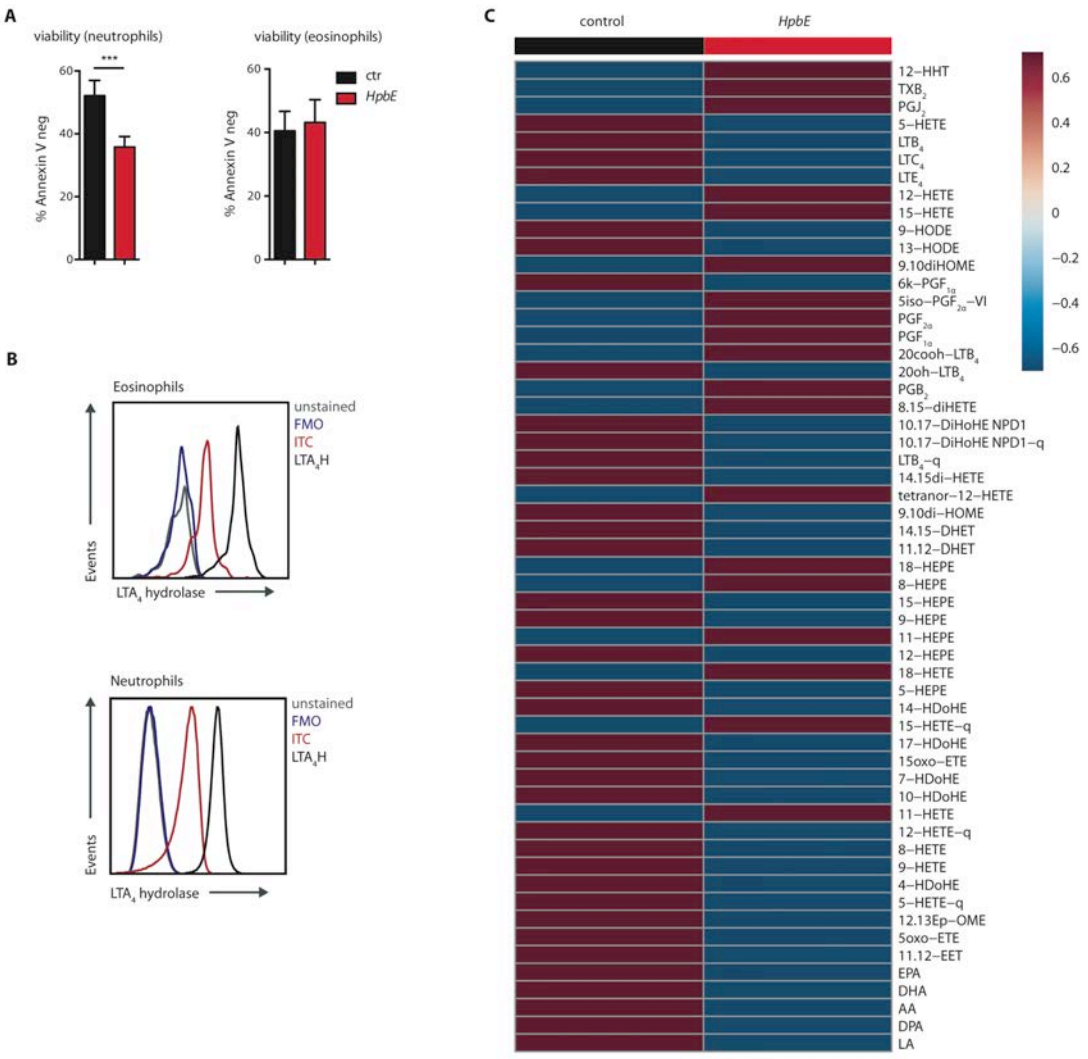

Fig. S4. Viability and LTA4H expression in human eosinophils and neutrophils and heat map of PUFA metabolites produced by human PMN in response to treatment with *HpbE*

(**A**) Viability of human neutrophils or eosinophils ± *HpbE* (24h). (**B**) Representative histograms showing intracellular LTA4H staining in human eosinophils or neutrophils from healthy blood donors compared to control stainings (FMO: fluorescence minus one, ITC: isotype control antibody). (**C**) LC-MS/MS data are shown as average z-scores for PMN from n=9 healthy human blood donors ± *HpbE*

(24h) + A23187 (10 min). Results in (A) are expressed as mean ± SEM, n=11 per group. Statistical significance was determined by Wilcoxon test. ***p < 0.001.

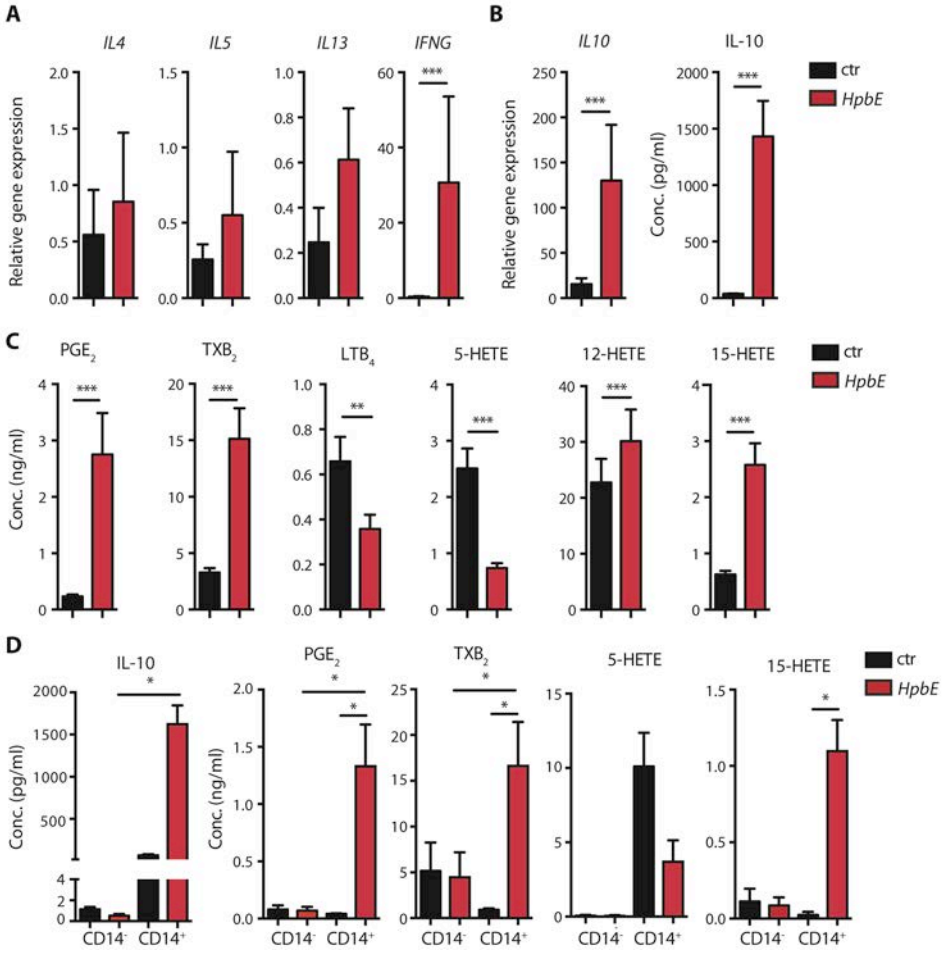

Fig. S5. *HpbE* induces a regulatory eicosanoid- and cytokine profile in mixed and isolated CD14$^+$ human PBMCs.

(**A**) Gene expression of type 2 cytokines or *IFNG* (qPCR) in human PBMCs ± treatment with *HpbE*. (**B**) Gene expression (qPCR) and protein levels (ELISA) of IL-10 in human PBMCs ± treatment with *HpbE*. (**C**) Levels of major eicosanoids (LC-MS/MS) produced by human PBMCs ± treatment with *HpbE* (24h) + A23187 (10 min). (D) Levels of IL-10 (ELISA) or eicosanoids (LC-MS/MS) produced by CD14$^-$

or CD14^{+} PBMCs ± treatment with *HpbE*. Data are presented as mean ± SEM, n=4-6 PBMCs from healthy human blood donors. Statistical significance was determined by Wilcoxon test (two groups) or Friedman test (more than two groups). *p<0.05, **p<0.01, ***p<0.001.

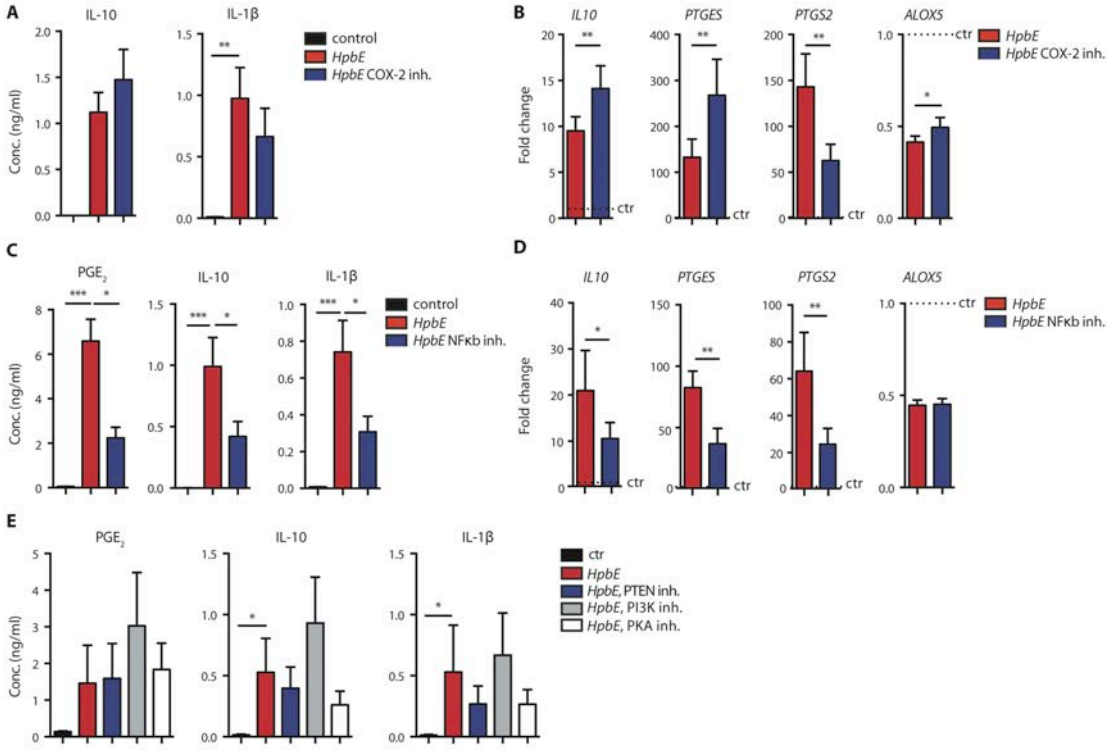

Fig. S6. Effect of COX-2-, NFκb-, PI3K-, PTEN- or PKA- inhibition on *HpbE*-driven modulation of cytokines and eicosanoid pathways

(**A**) Levels of IL-10 or IL-1β (ELISA) produced by human MDM ± treatment with *HpbE* ± selective COX-2 inhibitor (10 μM CAY10404). (**B**) Gene expression of *IL10*, PGE_2-synthetic enzymes or *ALOX5* (qPCR) for MDM treated with *HpbE* ± selective COX-2 inhibitor (CAY10404). (**C**) Levels of PGE_2 (EIA) or IL-10 and IL-1β (ELISA) for MDM ± treatment with *HpbE* ± NFκb inhibitor (5 μM BAY 11-7085) (24h) + A23187 (10 min). (**D**) Gene expression of *IL10*, PGE_2-synthetic enzymes or

ALOX5 (qPCR) for human MDM treated with *HpbE* ± NFκb inhibitor (BAY 11-7085). (**E**) Levels of PGE_2 (EIA) or IL-10 and IL-1β (ELISA) produced by human MDM after treatment with *HpbE* ± inhibitors of PTEN (250 nM SF1670), PI3K (100 nM Wortmannin) or PKA (10 µM H-89) (24h) + A23187 (10 min). Data are presented as mean ± SEM, MDM from n=5-11 donors. Statistical significance was determined by Wilcoxon test (two groups) or Friedman test (more than 2 groups). *p<0.05, **p<0.01, ***p<0.001.

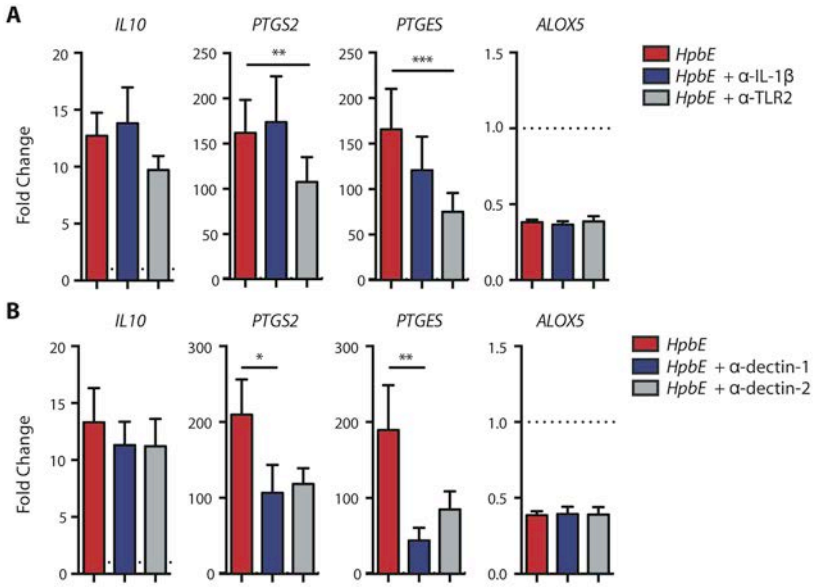

Fig. S7. Effect of neutralizing antibodies against PRRs (TLR2 and dectins-1 and -2) or IL-1β on *HpbE*-driven modulation of eicosanoids and IL-10.

(**A**) Relative gene expression of *IL10*, PGE_2-synthetic enzymes or *ALOX5* (qPCR) in human MDM treated with *HpbE* ± blocking antibodies against IL-1β (5 µg/ml) or TLR2 (10 µg/ml). (**B**) Relative gene expression of *IL10*, PGE_2-synthetic enzymes or *ALOX5* (qPCR) in human MDM treated with *HpbE* ± blocking antibodies against dectins-1 or -2 (10 µg/ml). Data are presented as mean ± SEM, MDM from n=5-8

donors. Statistical significance was determined by Wilcoxon test (two groups) or Friedman test (more than 2 groups). *p<0.05, **p<0.01, ***p<0.001. Dashed line indicates control level.

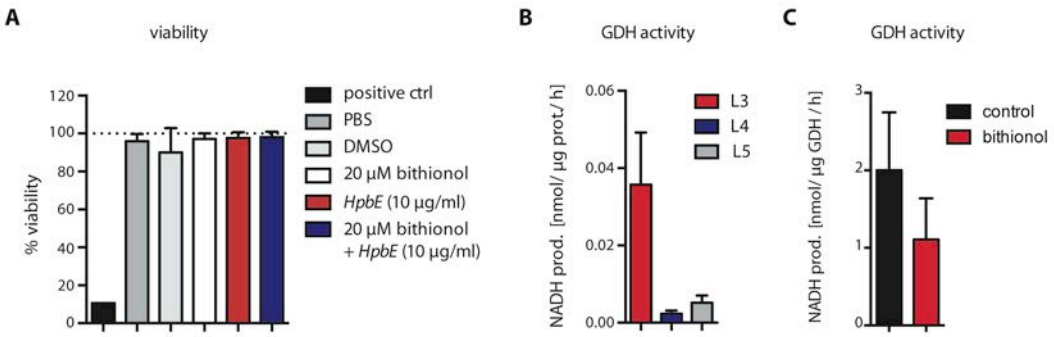

Fig. S8. Bithionol partially inhibits GDH activity, but does not affect cell viability and L3 stage *HpbE* shows a higher GDH activity as compared to L4 or L5 extracts.

(**A**) Viability (determined by LDH assay) of human MDM from n=3 healthy blood donors treated with DMSO, *HpbE* ± Bithionol as indicated. (**B**) GDH activity in L3, L4 or L5 extracts of *Hpb* (10 µg/ml) (n=2-4) in a GDH activity assay. (**C**) Effect of bithionol on the activity of recombinant *Hpb* GDH (n=2).

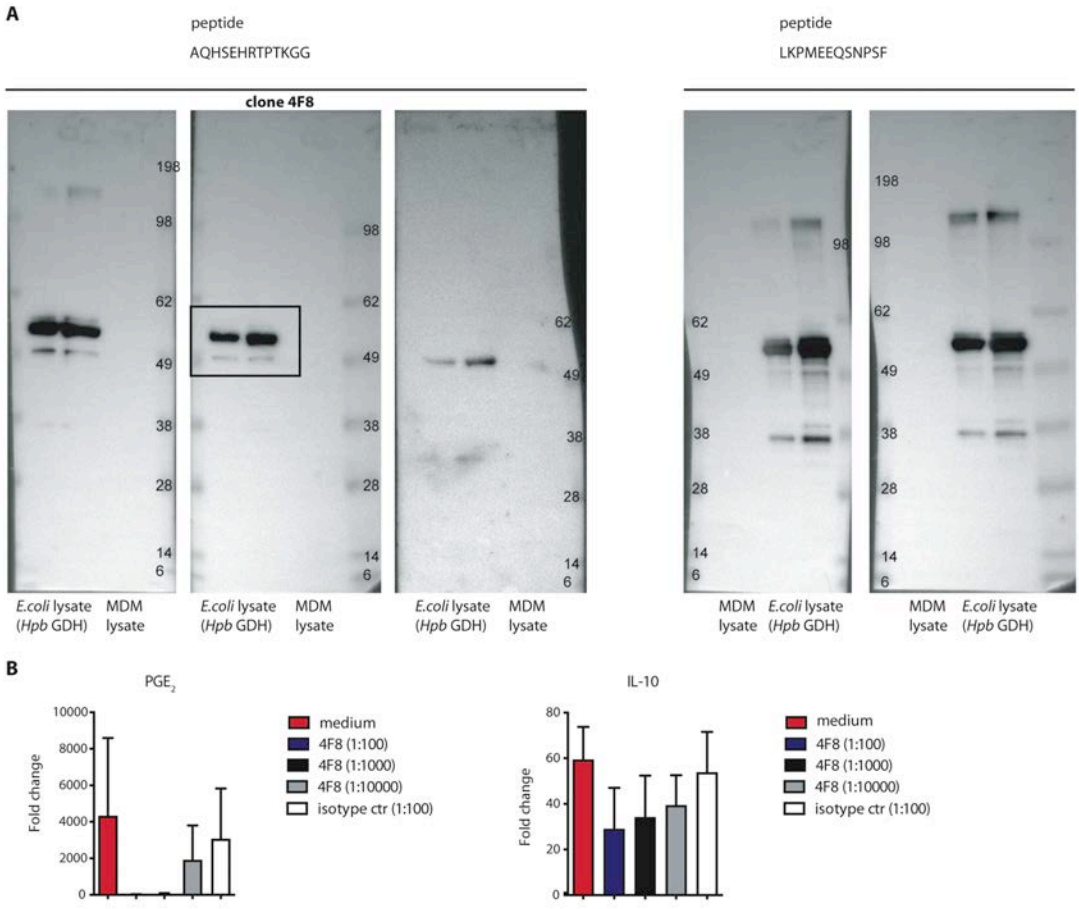

Fig. S9. Newly generated monoclonal antibodies recognize *Hpb* GDH and clone 4F8, but not an isotype control antibody reduces *HpbE*-induced PGE_2 and IL-10 production.

(**A**) A lysate from *E. coli*, overexpressing *Hpb* GDH (lanes 1 and 2 on the left for peptide AQHSEHRTPTKGG; lanes 2 and 3 on the right for peptide LKPMEEQSNPSF) or a lysate of human MDM (lane 3 on the left; lane 1 on the right) were probed with newly generated monoclonal antibodies against *Hpb* GDH (peptides used for immunization are specified above the blots). Clone 4F8 was chosen for further subcloning and neutralization experiments. (**B**) Levels of PGE_2 (EIA) or IL-10 (ELISA) induced by *HpbE* treatment of human MDM (relative to

untreated cells) in the absence (medium) or presence of clone 4F8 or an isotype control antibody at the indicated dilutions. Data are presented as mean ± SEM, MDM from n=3 donors.

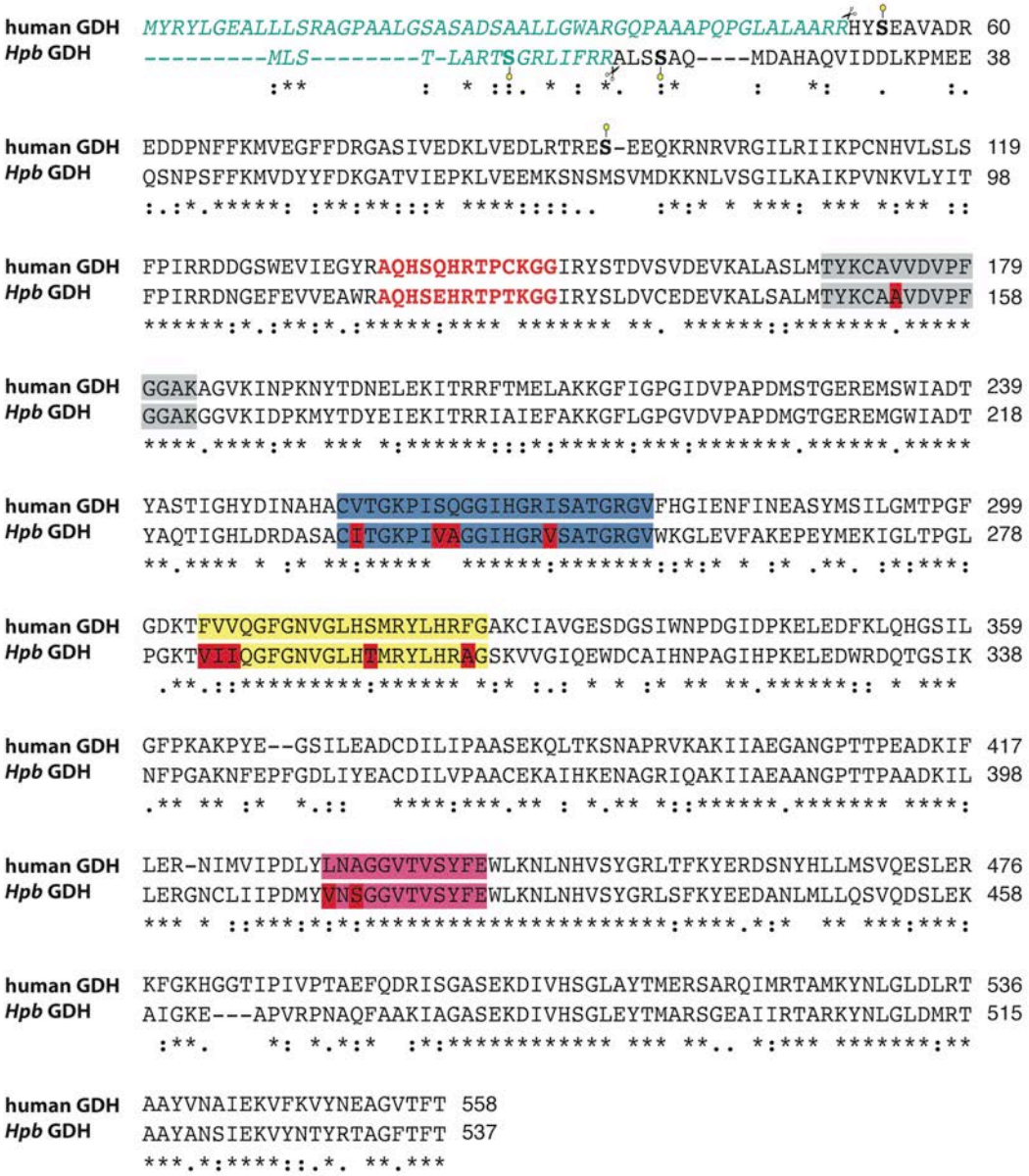

Fig. S10. Sequence of *Hpb* GDH is distinct from human GDH and contains potential predicted glycosylation sites.

Sequence alignment of human GDH and *Hpb* GDH prepared by Clustal Omega. Glutamate/phenylalanine/leucine/valine dehydrogenase catalytic centers are highlighted in different colors (grey, blue, yellow and pink). Amino acid exchanges of *Hpb* GDH compared to human GDH inside the catalytic centers are marked in red. The asterisk (*) indicates conserved residues. The colon indicates conservation of groups between strongly similar properties, whereas the period (.) indicates conservation between groups of weakly similar properties.

The binding site of the anti-*Hpb* GDH antibody (4F8) is highlighted in red. Mitochondrial targeting sequences are shown in italic and predicted O-glycosylation sites (identified by NetOGlyc 4.0 Server) in bold and with yellow sugar moieties.

Supplementary tables

Table S1. LC-MS/MS panel of PUFAs and PUFA metabolites

(See separate excel file)

Table S2. Proteins present in active fractions of *HpbE* identified by mass spectrometry

(See separate excel file)

	Gene	Forward primer sequence (5' – 3')	Reverse primer sequence (5' – 3')
Human			
Housekeeper	***GAPDH***	GAAGGTGAAGGTCGGAGT	GAAGATGGTGATGGGATTTC
LOX pathway	***ALOX5***	GATTGTCCCCATTGCCATCC	AGAAGGTGGGTGATGGTCTG
	LTA4H	CAGTGGCTCACTCCTGAACA	TCTGGGTCAGGTGTTTCTCC

	LTC4S	GACGGTACCATGAAGGACGA	GGAGAAGTAGGCTTGCAGCAG
	CYSLTR1	CAGTGGACGCTTTGATCTTA	AAGCTTGTCCACGCATATTA
COX pathway	***PTGS2***	GCTGGAACATGGAATTACCCA	CTTTCTGTACTGCGGGTGGAA
	PTGES	TCAAGATGTACGTGGTGGCC	GAAAGGAGTAGACGAAGCCCAG
	PTGDS	CCCAGGGCTGAGTTAAAGGA	AGAGCAGAGACATCCAGAGC
M2 markers	***ALOX15***	GGACACTTGATGGCTGAGGT	GTATCGCAGGTGGGGAATTA
	MRC1	CGATCCGACCCTTCCTTGAC	TGTCTCCGCTTCATGCCATT
	TGM2	AGGCCCGTTTTCCACTAAGA	AGCAAAATGAAGTGGCCCAG
Type 2 cytokines	***IL4***	GTGTCCTTCTCATGGTGGCT	CAGACATCTTTGCTGCCTCC
	IL5	TCTCCAGTGTGCCTATTCCC	CGAACTCTGCTGATAGCCAA
	IL13	GATTCCAGGGCTGCACAGTA	GGTCAACATCACCCAGAACC
	IFNG	TCAGCCATCACTTGGATGAG	CGAGATGACTTCGAAAAGCTG
	IL10	CTCATGGCTTTGTAGATGCCT	GCTGTCATCGATTTCTTCCC
Mouse			
Housekeeper	***Gapdh***	GGGTGTGAACCACGAGAAAT	CCTTCCACAATGCCAAAGTT
LOX pathway	***Alox5***	ATTGCCATCCAGCTCAACCA	ACTGGAACGCACCCAGATTT
	Ltc4s	ATCTTCTTCCACGAAGGAGCC	TCGCGTATAGGGGAGTCAGC
COX pathway	***Ptgs2***	GGGCCATGGAGTGGACTTAAA	TCCATCCTTGAAAAGGCGCA
	Ptges	GAAGAAGGCTTTTGCCAACCC	TCCACATCTGGGTCACTCCT
M2 markers	***Arg1***	GCAACCTGTGTCCTTTCTCC	TCTACGTCTCGCAAGCCAAT
	Tgm2	TAAGAGTGTGGGCCGTGATG	TTTGTTCAGGTGGTTGGCCT
	Mrc1	TTGCACTTTGAGGGAAGCGA	CCTTGCCTGATGCCAGGTTA
	Tmed1* / *St2l	AGTAGAGGGTGACCCGGATG	GAACTCGCCGTCCTGGATAG
	Retnla* / *Fizz1	GGGATGACTGCTACTGGGTG	TCAACGAGTAAGCACAGGCA

Table S3: Primer sequences for qPCR.

REAGENT or RESOURCE	SOURCE	IDENTIFIER
Antibodies		
Donkey anti-goat IgG (H+L) cross-adsorbed secondary antibody, Alexa Fluor 568, RRID AB_2534104	Thermo Fisher Scientific	Cat#A-11057
Donkey anti-rabbit IgG (H+L) cross-adsorbed secondary antibody, Biotin, RRID AB_228212.	Thermo Fisher Scientific	Cat#31821
Donkey anti-rabbit IgG (H+L) highly cross-adsorbed secondary antibody, Alexa Fluor 647, RRID AB_228212	Thermo Fisher Scientific	Cat#A-31573
Donkey anti-rat IgG (H+L) highly cross-adsorbed secondary antibody, Alexa Fluor 488, RRID AB_2535794	Thermo Fisher Scientific	Cat#A-21208
Goat anti-human COX-2 affinity-purified polyclonal Antibody	Cayman Chemical	Cat#100034
Goat anti-human LTA4 hydrolase (C-21) affinity-purified polyclonal antibody	Santa Cruz Biotechnology	Cat#sc-23070
Mouse anti-human β-actin monoclonal antibody (AC74)	Sigma-Aldrich	Cat#A2228
Mouse anti-human CD193 (CCR3) (5E8) monoclonal antibody, BB700	BD Biosciences	Cat#745843
Mouse anti-human Dectin-1 neutralizing monoclonal antibody	Invivogen	Cat#mabg-hdect
Mouse anti-human Dectin-2 neutralizing monoclonal antibody	Invivogen	Cat#mabg-hdect2
Mouse anti-human IL-1β (8516.311) neutralizing monoclonal antibody	Abcam	Cat#ab10749
Mouse anti-human TLR2 neutralizing antibody	Invivogen	Cat#maba2-htlr2
Rabbit anti-human HIF-1α (C-Term) polyclonal antibody	Cayman Chemical	Cat#10006421
Rabbit anti-human LTC4 synthase (S-18)-R affinity-purified polyclonal antibody	Santa Cruz Biotechnology	Cat#sc-22564-R
Rabbit anti-human p38 MAPK (D13E1) XP® monoclonal antibody	Cell Signaling Technology	Cat#8690
Rabbit anti-human phospho-p38 MAPK (Thr180/Tyr182) (D3F9) XP® monoclonal antibody	Cell Signaling Technology	Cat#4511
Rat anti-human CD294 (CRTH2) (BM16) monoclonal antibody, PE-CF594	BD Biosciences	Cat#563501
Rat anti-mouse F4/80 monoclonal antibody (BM8), RRID AB_467558	Thermo Fisher Scientific	Cat#14-4801-82
Bacterial and Virus Strains		
Bacillus cereus	Prof. Clarissa Prazeres da Costa, Technical University of Munich, Germany (This paper)	N/A
Enterococcus faecalis		
Paenibacillus odorifer		
Stenotrophomonas maltophilia		
Biological Samples		
Human blood cells	Center of Allergy & Environment, Technical University of Munich, Germany	N/A
Patient nasal polyp tissues	Department of Otolaryngology, Klinikum rechts der Isar, Technical University of Munich, Germany	N/A
Chemicals, Peptides, and Recombinant Proteins		

3,3′-Diaminobenzidine (DAB) Enhanced Liquid Substrate System tetrahydrochloride	Sigma-Aldrich	Cat#D3939
Acriflavine	Sigma-Aldrich	Cat#A8126
BAY 11-7085	Enzo Life Sciences	Cat#BML-EI279-0010
Calcium Ionophore A23187	Sigma-Aldrich	Cat#C7522
CAY10404	Cayman Chemical	Cat#70210
Dexamethasone	Sigma-Aldrich	Cat#
Fluticasone propionate	Sigma-Aldrich	Cat#F9428
H-89	Cayman Chemical	Cat#10010556.5
HDM extract from *Dermatophagoides farinae*	Stallergenes SA	N/A
LPS	Invivogen	Cat#tlrl-eblps
Human GM-CSF	Miltenyi Biotech	Cat#130-093-867
Human IL-8	Miltenyi Biotec	Cat#130-093-942
Human RANTES	Miltenyi Biotec	Cat#130-093-989
Human TGF-β1, human	PeproTech	Cat#100-21C
Indomethacin	Cayman Chemical	Cat#70270
Leukotriene B_4	Cayman Chemical	Cat#420114
Montelukast	Cayman Chemical	Cat#10008318
Mouse GM-CSF	Miltenyi Biotech	Cat#130-095-793
SF1670	Cayman Chemical	Cat#15368.1
VX-702	Cayman Chemical	Cat#13108
Wortmannin	Cayman Chemical	Cat#10010591.1
Critical Commercial Assays		
Bioplex Pro Reagent Kit V	Bio-Rad	Cat#12002798
Cysteinyl Leukotriene ELISA Kit	Cayman Chemical	Cat#500390
Human IL-10 ELISA Set	BD Biosciences	Cat#555157
Human IL-1β ELISA Set II	BD Biosciences	Cat#557953
Leukotriene B4 ELISA Kit	Cayman Chemical	Cat#520111
Magnetic Luminex Assay	R&D Systems	Cat#LXSAHM-17
Prostaglandin E2 ELISA Kit	Cayman Chemical	Cat#514010
Thromboxane B2 ELISA Kit	Cayman Chemical	Cat#501020
GDH activity assay kit	Sigma-Aldrich	Cat#MAK099
Deglycosylation kit	Sigma-Aldrich	Cat# EDEGLY
LDH Cytotoxicity Assay kit	Thermo Scientific	Cat#88953
Experimental Models: Cell lines		
Primary bone marrow-derived macrophages	WT C57BL/6, HIF-$1\alpha^{floxed/floxed}$ x LysMCre, *PTGS2*$^{-/-}$, PTGES$^{-/-}$	N/A
Monocyte-derived macrophages Peripheral blood mononuclear cells Polymorphonuclear leukocytes	Human blood, Center of Allergy & Environment, Klinikum rechts der Isar Technical University of Munich, Germany (Dietz et al., 2016)	N/A
Experimental Models: Organisms/Strains		
Mouse: BALB/c	Charles River Laboratories	N/A
Mouse: C57BL/6	École Polytechnique Fédérale de Lausanne (EPFL), Switzerland	N/A

Mouse: C57BL/6J	Charles River Laboratories	N/A
Mouse: HIF-1α$^{floxed/floxed}$ (C57BL/6J background)	Prof. Bernhard Brüne, Goethe-University Frankfurt, Germany (Scheerer et al., 2013)	N/A
Mouse*: PTGS2*$^{-/-}$ (C57BL/6J background)	Prof. Rolf Nüsing, Goethe-University Frankfurt, Germany (Vegiopoulos et al., 2010)	N/A
Mouse*: PTGES*$^{-/-}$ (C57BL/6J background)	Prof. Per-Johan Jakobsson, Karolinska Institute Stockholm, Stockholm, Sweden (Trebino et al. 2003)	N/A
Heligmosomoides polygyrus bakeri	Prof. Nicola Harris, École Polytechnique Fédérale de Lausanne (EPFL), Lausanne, Switzerland; Prof. David Voehringer, Friedrich-Alexander University, Erlangen-Nuremberg, Germany (Camberis et al., 2003)	N/A
Schistosoma mansoni	Prof. Clarissa Prazeres da Costa, Technical University of Munich, Germany, (Ritter et al., 2010)	N/A
Oligonucleotides		
Primers for quantitative real-time PCR experiments	This paper	see Table S1
Software and Algorithms		
FlowJo v10 software	FlowJo LLC	www.flowjo.com
GraphPad Prism version 6	GraphPad Software	www.graphpad.com
MetaboAnalyst version 3.0	Mc Gill University, Quebec, Canada	www.metaboanalyst.ca
Other		
EVOS™ FL Auto Imaging System	Thermo Fisher Scientific	N/A
BD LSRFortessa™	BD Biosciences	N/A
Leica SP5 confocal microscope	Leica Microsystems	N/A
LC-MS/MS: Agilent 1290 coupled to QTRAP 5500	Agilent/ AB Sciex	N/A

Table S4: Reagents and resources.